GEOCHEMISTRY OF MAFIC GRANULITES FROM ANIYAPURAM MAFIC-ULTRAMAFIC COMPLEX (CAUVERY SUTURE ZONE) SOUTHERN INDIA: IMPLICATIONS FOR SUPRASUBDUCTION ZONE TECTONICS

T. Yellappa

Senior Scientist, Geochemistry Division
CSIR-National Geophysical Research Institute, Hyderabad-500007, India

Abstract: ***The granulite facies rocks of Southern Granulite Terrain (SGT), India represent lower crust-upper mantle products of different tectonothermal events in different origins. They include charnockites, two pyroxene granulites of mafic-felsic, dismembered ophiolite sequence, mafic-ultramafic intrusions and granitoids. The southern part of the Cauvery Suture Zone (CSZ) around Aniyapuram-Mohanur, near Namakkal is dominated by wide range of mafic-felsic granulites. These are well exposed in close association with dismembered mafic and ultramafic rocks including peridotite, pyroxenite, amphibolite, gabbro-gabbronoritic rocks metapelite, metachert with younger intrusives of pegmatite and granitoids. The petrology of these granulites are characterized by sub-idioblastic fine to coarse-grained clinopyroxene (40-50%) and orthopyroxene (10-20%), idioblastic garnets (20-30%), subhedral to anhedral amphiboles (10-20%) and plagioclases (5%) with accessory phases of apatite, zircon, biotite and opaque minerals. Whole rock geochemistry of 14 representative samples reveal, the granulites are mafic to slightly intermediate in composition with higher SiO_2 (47-53 wt%) and $A1_2O_3$ (10-16 wt%) with low K_2O contents (<0.4wt%). Trace element ratios are extremely variable with very high K/Rb ratios (540-13447) reflected in very low Rb contents (0.2-7 ppm) and varied Ba/La (1.8-43.40), Rb/Sr (0.0001-0.13) and Sr/Nd (3.23-34.25) concentrations. The geochemical variation plots ($Na_2O+K_2O-FeO_t$-MgO and Zr vs. Y) reveal that these granulites belong to calc-alkaline to tholeiitic signatures. On various tectonic discrimination plots (MnO-TiO_2-P_2O_5, Ti vs. V, Ti vs. Zr, and Cr vs. Y) these show island arc origin. Spider diagrams with normalized MORB show enrichment of LILE (Sr, K, Rb, Ba) and depletion of HFSE (Ti, Nb, Ta, Hf) with -ve Nb anomalies. The above results with available age data suggest that the protoliths of the mafic granulites are tholeiitic basalts developed in island arc environment related to Neoarchean to Paleoproterozoic suprasubduction zone tectonic setting, consistent with dismembered ophiolite sequence of this region and have been subjected to granulite facies metamorphism during Neoproterozoic arc magmatism in the terrain.***

Key words: Mafic granulites, Island arc, Suprasubduction zone, Cauvery Suture Zone, Southern Granulite Terrain.

1. INTRODUCTION

Granulite facies rocks are important candidates for the study of metamorphic and exhumation processes and is an indicator of high-grade metamorphism and deep-seated ductile deformation (Bohlen and Mezger, 1989). These rock types are commonly considered as major constituents of the lower continental crust and has a link with orogenic events in terms of their evolution of four important periods of Earth history: Archean-Paleoproterozoic (2.7-2.45 Ga), Mid-Paleoproterozoic (2.0-1.8 Ga), Late- Mesoproterozoic to early Neoproterozoic (1.4-1.0 Ga) and Late Proterozoic to Cambrian (0.63-0.51Ga) in association with major supercontiental evolution (Brown, 2007). The common origin these high grade metamorphic (granulite facies) rocks are from mid to lower (20-30 km) continental crust (Christensen and Fountain, 1975) in a temperature range of 700-1000^{0}C and pressure range of 6-10 kbars. The occurrence of these granulite facies rocks were described in variety of tectonic settings. The typical among them are Precambrian regional belts exposed in continental shield areas from hundreds to thousands of square kilometer areas. Such basement complexes are often relatively uniform grade, but also shows variation towards amphibolite facies conditions (Hansen *et al.,* 1984) or exhibit regional thermo barometric variations (Harley, 2004).

The granulite terrains are generally comprised of several rock types that include varied suites such as mafic-ultramafic, felsic orthogneisses, migmatites, charnockites and paragneisses derived from pelite, siliceous and calcareous precursors (Percival, 1994). Those terrains, in which some partial melting has taken place at high-grade metamorphism contemporaneously with overlapping deformation and are structurally complex in understanding. Such rocks are later exhumed on to the surface by tectonic processes such as collision-accretion of various crustal blocks from Neoarchean to Neoproterozoic periods (Harris *et al.,* 1994). The Southern Granulite Terrain (SGT) of the Indian shield, the Kapuskasing structural zone of Canada and the Arunta Block of Australia are a few typical examples of Neoarchean-Neoproterozoic high-grade granulite terrains in the world (Percival, 1994). Among these several granulite terrains were also described in Proterozoic and Phanerozoic collisional belts such as the Aravalli-Delhi fold belt and the Eastern Ghats Mobile Belt in India, the Grenville Front Tectonic Zone (USA), the Alps of Europe and the Himalayas of Asia.

Precambrian granulite-gneissic terrains may represent exhumed root zones of ancient orogenic belts provide the motivation for detailed studies on these terrains. The Southern Indian Shield, for long considered that the granulite-gneissic terrain as a single composite terrain entity developed around Dharwar craton. It is not only preserves the important records of lower crustal processes and lithospheric geodynamics, but also carry imprints of the tectonic framework related to the assembly of supercontinents: Rodinia and Gondwana (Santosh *et al.*, 2009; Collins *et al.*, 2007; Collins *et al.*, 2014). This terrain exposes the windows of middle to lower crust with well-preserved rock records displaying multiple tectonothermal events and multiphase exhumation paths (Ghosh *et al.*, 2004; Brandt *et al.*, 2014; Collins *et al.*, 2014). The Cauvery Suture Zone (CSZ) in the southern granulite terrain is a major tectonic boundary in the terrain which separates the

Neoarchean granulite belt block to the north and the Neoproterozoic Madurai granulite block to the south (Fig.1a). It is generally regarded as a dextral crustal- scale shear zone trending in E-W connecting Ranostara suture in Madagascar. The CSZ is also described as an ancient suture zone with oceanic remnants and ultra-high temperature rocks and has attracted the attention of many national and international groups in recent years because of its significance in the supercontinental reconstruction models (Drury *et al.,* 1984; Ramakrishnan, 1993; Gopalakrishnan, 1994; Santosh *et al.,* 2009; Brandt *et al.,* 2014; Collins *et al.,* 2014; Glorie *et al.,* 2014; Chetty *et al.,* 2016). Recently three important Neoarchean to Nepoproterozoic ophiolite complexes have been described from the CSZ including the Manamedu Ophiolite Complex (MOC), occurring at the northern bank of the Cauvery river course, Devanur Ophiolitic Complex (DOC), located about 20km north of MOC and Agali Hill Ophiolite Complex (AOC) in the western boundary of the shear zone near Attapadi (Fig.1a; Yellappa *et al.,* 2010, 2012; Santosh *et al.,* 2013). All the three complexes comprises disremembered sequence of mafic-ultramafic group of rocks including dunites, peridotites, pyroxenites, gabbro, gabbro norite, anorthosite, sheeted mafic dykes, amphibolite to andesite categories and plagiogranites/trondhjemites with a thin pile of ferruginous cherts. Based on geochemical characteristics of these complexes, these have been described that they developed at shallow levels from mantle-derived arc magmas within a suprasubduction zone tectonic setting (Yellappa *et al.,* 2010, 2012; Santosh *et al.,* 2013).

The present study focused on similar dismembered complex called Aniyapuram Mafic-Ultramafic Complex (AMUC) occurs within the CSZ near Mohanur, Namakkal district. Based on the geochemistry of mafic rocks from the complex and Pb-Pb dating of zircons from metagabbro, it is described that the protolith was evolved during Neoarchean-Paleoproterozoic periods under suprasubduction zone tectonics and metamorphosed during middle to Neoproterozoic periods (Koizumi *et al.,* 2014; Yellappa *et al.,* 2014). This paper presents some new results on mafic granulites of this complex and their mineral assemblages, geochemical features and tectonic history of their evolution. These data, together with other geological observations including age, P-T studies, allow us to describe possible explanation for the nature of origin of protolith of mafic granulitic rocks associated with suprasubduction tectonics.

2 REGIONAL GEOLOGY

The Southern granulite terrain (SGT) extends from 8^0 to 11^0 N latitude of India (Tamil Nadu, Karnataka, and Kerala states) and it is one of few terrains of the world with preservation of Archean-Proterozoic crust of extensive high-grade granulite facies rocks. The terrain is believed to be of lower crustal origin through a complex evolutionary history with multiple deformations, anatexis, several intrusions and polyphase metamorphic events (Ghosh *et al.,* 2004; GSI, 2006; Ramakrishnan and Vaidyanathan, 2008; Santosh *et al.,* 2009; Collin *et al.,* 2014). More than 80% of the terrain is covered by varied lithologies of Archean and Proterozoic age groups namely, Sathyamangalam Group (>3200 Ma), layered mafic and ultramafic complexes, Bhavani Group (~3000 Ma), Kolar Group (~2900 Ma), Khondalite Group, Charnockite Group (~2600-800 Ma) and Migmatitic complex (2200-2250Ma) younger Proterozoic granitoids (~550Ma) and etc., (GSI, 2006). The Proterozoic rocks include younger granulites/charnockites, mafic and ultramafic rocks, alkali syenites, carbonatites and granites mostly occur in and around the Cauvery Suture Zone and its south (CSZ, GSI, 2006).

The terrain has been divided into a number of distinct crustal blocks (Fig. 1a) based on the structural and isotopic evolution from north to south: (1) Northern block (2) the Nilgiri Block (3) the Salem-Madras Block, (4) the Madurai Block, (5) the Trivandrum Block and (6) the Nagercoil Block (Santosh *et al.,* 2009; Plavsa *et al.,* 2012; Collins *et al.,* 2014). The Northern and Nilgiri Blocks made up of migmatized garnetiferrous rocks, enderbitic granulites, charnockite massifs with kyanite-bearing gneisses, quartzites and metabasites (Janardhan *et al.,* 1994). The Salem-Madras Block exposed with orthogneisses, charnockites, mafic granulite and ultramafic intrusions in association with metasedimentary units, a succession that continues up to the Palghat-Cauvery Shear Zone (PCSZ), also termed as Cauvery Suture Zone (Goplakrishnan, 1994; Collins *et al.,* 2007). The Madurai Block occurs immediately south of the suture zone (CSZ) and one of the largest crustal block in southern India, comprises dominantly of charnockite massifs intercalated with tonalitic/ granodioritic gneisses and elongated narrow belts and slivers of metasedimentary rocks including quartzites, metamorphosed carbonates, iron formations and pelites, suggesting an accretionary realm (Santosh *et al.,* 2009). The southern margin of the Madurai Block is marked by the Achankovil Shear Zone (AKSZ), separates the Madurai Block from the Trivandrum Block to the south. The Trivandrum Block is further classified as the Kerala Khondalite Belt (KKB), the Nagercoil Achankovil metasediments based on lithological grounds. Trivandrum and Nagercoil Blocks consists of dominantly metasedimentary gneisses, garnet-bearing felsic gneisses (known locally as leptynites) and granulite facies of garnet+spinel+cordierite+sillimanite metapelites (termed khondalites). Calc-granulites, quartzites and ultramafic rocks also occur as linear bodies along the local structural trends. These lithologies of Kerala Khondalite Belt (KKB) described as a sequence of continental margin sediments (Chacko *et al.,* 1987).

The terrain broadly witnessed by two events of granulite facies metamorphism: Neoarchean (ca. 2.5 Ga) cratonic part in the north and Neoproterozoic (ca 1.0–0.55 Ga) terrain in the south. There are several studies on the high grade metamorphism and associated rocks from the terrain: the charnockites from Pallavaram and Shevroy hill massifs described as quartz- K-feldspar-plagioclase feldspar-clinopyroxene- garnet- hornblende- biotite- apatite- zircon- magnetite- ilmenite- rutile- pyrope association (Rajesh and Santosh, 2004). However, the mafic charnockites from the Shevroy hill massif has plagioclase- clinopyroxene- orthopyroxene- hornblende- magnetite-ilemenite- rutile- K-feldspar- biotite- apatite- zircon. The non-garnetiferous enderbites from both the Biligirirangan and Nilgiri hill massifs show similar mineralogy of quartz- plagioclase- feldspar- clinopyroxene- garnet- hornblende-biotite- apatite- zircon- magnetite- ilmenite-rutile- pyrope. The felsic type of Cardamom hill massif has dominant mineralogy of quartz- K-feldspar- plagioclase feldspar- orthopyroxene-magnetite- ilmenite- apatite, - hornblende- biotite while the intermediate type Cardamom hill massif has mineralogy of quartz- plagioclase-K-feldspar- orthopyroxene- clinopyroxene- hornblende- biotite- magnetite- rutile- zircon- apatite. The Nagercoil massif charnockites consist of quartz- plagioclase- K-feldspar- orthopyroxene- clinopyroxene- hornblende- biotite-magnetite- rutile- zircon- apatite- garnet mineral assemblage (Rajesh and Santosh, 2004).

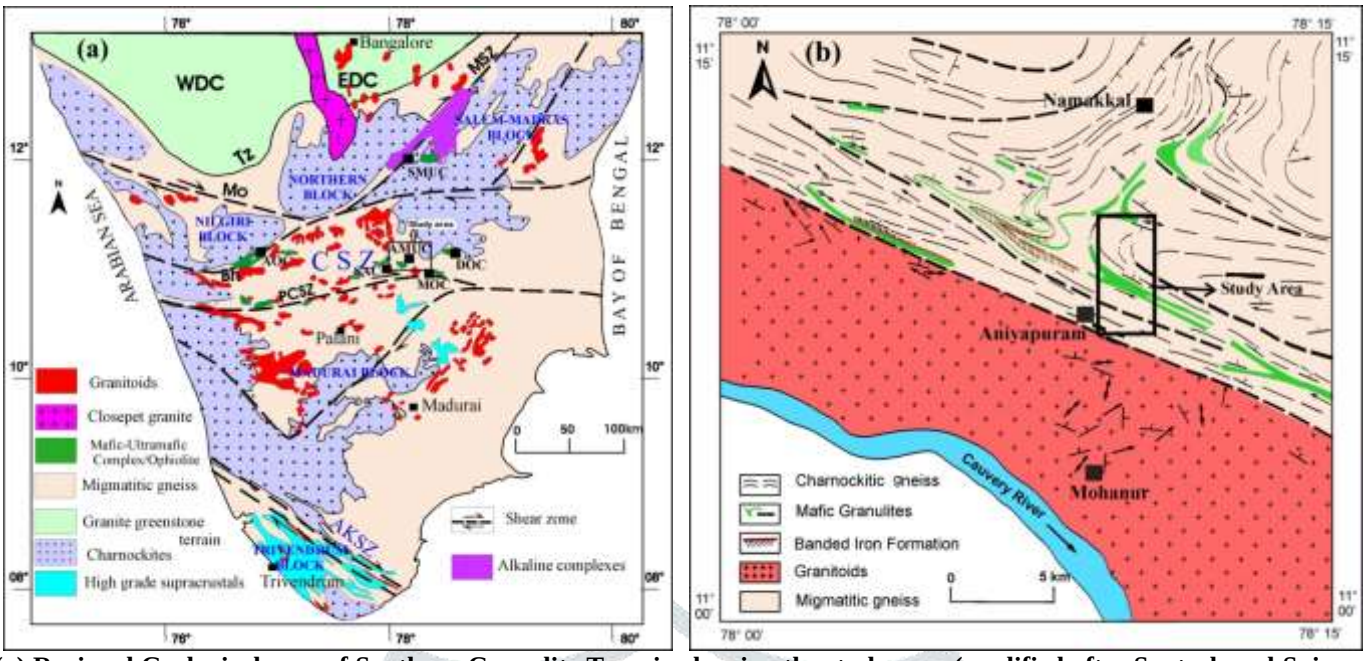

Fig. 1: (a) Regional Geological map of Southern Granulite Terrain showing the study area (modified after Santosh and Sajeev, 2006 and source from Geological Survey of India maps), Mo-Moyar, Bh-Bhavani, PCSZ-Palghat-Cauvery Shear Zone, MSZ Moyar Shear Zone, CSZ-Cauvery Suture Zone, AKSZ-Achankovil Shear Zone, WDC-Western Dharwar Craton, EDC-Eastern Dharwar Craton, Tz-Transition Zone, SAC-Sittampundi Anorthosite Complex, SMUC-Salem Mafic and Ultramafic Complex, AMUC-Aniyapuram Mafic and Ultramafic Complex, DOC-Devanur Ophiolite Complex, MOC-Manamedu Ophiolite Complex; (b) Structural map of the Namakkal-Mohanur corridor in the CSZ derived from Landsat images showing different lithological assemblages and structural trends (after Yellappa et al., 2014).

The CSZ is a crustal-scale (suture) shear zone system divides the Southern granulite terrain (SGT) of southern India into two discrete tectonic blocks (Drury and Holt, 1980; Gopalakrishnan, 1994). The most prominent feature of this is an east-west trending zone of intense planar fabrics separating the northern Neoarchean granulite block(s) from the Neoproterozoic Madurai granulite block (MGB). The geology and the age relationships of the CSZ have been reviewed by several workers (Ghosh *et al.*, 2004; Plavsa *et al.*, 2012, 2014). The CSZ has been variously described as: (i) a collision zone and cryptic suture, evident from the occurrence of remnants of probable ophiolitic sequence (Gopalakrishnan, 1994), (ii) dextral shear zone as exemplified by the deflection of north-south Archean fabrics to near east-west disposition along the MBSZ (Drury *et al.*, 1984), (iii) an analogue of the central part of Limpopo mobile belt (Ramakrishnan, 1993), (iv) the Archean-Proterozoic Terrain boundary (Harris *et al.*, 1994), (v) a zone of Paleo- and Neoproterozoic reworking of Archean crust (Bhaskar Rao *et al.*, 1996) and (vi) a Neoproterozoic dextral-ductile transpressive tectonic zone (Chetty and Bhaskar Rao, 2006). It is also considered as the trace of the Cambrian suture zone of Gondwana (Collins *et al.*, 2007; Santosh *et al.*, 2009) represents several occurrences of Neoarchean to Neoproterozoic dismembered ophioilites (Santosh *et al.*, 2013; Yellappa *et al.*, 2010, 2012, 2014). There are several reports of granulite facies assemblages, such as orthopyroxene-bearing granulites, sapphirine-bearing pelites, and calc-silicate rocks, which suggest occurrence of high to ultra-high temperature metamorphism (e.g., Raith *et al.*, 1997). In the eastern part of the CSZ and in Madurai Granulite Block, several workers (e.g., Tsunogae and Santosh, 2006; Nishimiya *et al.*, 2010) have documented the evidence for prograde high-pressure (HP) events and subsequent ultra high-temperature (UHT) metamorphism along a clockwise path based on geochemical and petrological studies. In a recent study, Nishimiya et al. (2010) also reported equilibrium sapphirine + quartz assemblage from Panangad area within the CSZ providing unequivocal evidence for extreme crustal metamorphism at UHT conditions associated with the collisional assembly of the Gondwana supercontinent in the Neoproterozoic-Cambrian period. These results indicate peak UHT conditions of 940-990°C at 7-8 kbar followed by a retrograde event of 600-700°C along a clockwise *P-T* path (Santosh *et al.*, 2009). It is also documented the regtrogressed eclogites from the well known Sittampundi anorthosite complex of the garnet gabbro layer within the anorthosite suite (Sajeev *et al.*, 2009). The P-T conditions represent that garnet-rutile-melt was the peak metamorphic assemblage that eclogites developed at ca 20 kbar and above 1000^0C (Sajeev *et al.*, 2009).

3 METHODOLOGY

Geological mapping of the complex has been carried out in different scales to understand the lithological distributions and its style of deformation. Several structural measurements have been carried out and collected representative samples of different lithologies for petrological and geochemical studies in the laboratory. Selected samples have made thin sections and studied under microscope. After detailed study of their petrological features, 14 representative samples chosen for whole rock geochemistry. These samples were chipped manually and cleaned by ultrasonication using de-ionized water. The samples were crushed to coarse (<1 cm) edge length in a steel jaw crusher and pulverized to fine powder using steel and agate tools. Major element analysis was performed on pressed fine powder pellets, using Philips Magi X PRO-PW2440 X-ray fluorescence (XRF) spectrometer at NGRI, Hyderabad. For trace and rare earth elements, the sample solutions were prepared using standard procedures with a mixture of distilled HF +HNO_3 + $HClO_4$ + HCl acids in screw capped Savillex Teflon beakers. Rh is used as internal standard (Balaram and Rao, 2003). The analysis was performed with Perkin Elmer DRC-II ICP-MS at NGRI, Hyderabad. For the both XRF and ICP-MS, a range of synthetic element and international rock standard reference materials were applied for calibration.

4 RESULTS

4.1 Field characteristics of the complex

The study area falls in Namakkal area, north of Mohanur village and also it has been described as Namakkal-Mohanur Corridor (NMC, Fig. 1b). The area is exposed along the train cutting section with in the corridor over a length of ~6 kms between Namakkal and Mohanur, near Aniyapuram,. The complex is trending north-south nearly orthogonal to regional trend of the rocks exposed in the south central part of the CSZ. The important rock units in the region comprise mafic-ultramafic rocks, charnockitic rocks, hornblende gneisses, two-pyroxene granulites, migmatite gneiss, banded iron formations, cherty bands and the intrusives of younger granitoids. The AMUC represents a variety of lithological assemblages dominantly of mafic-ultramafic rocks and two pyroxene granulites. The ultramafic rocks include peridotites, hornblendites, pyroxenites, serpentinites and mafic rocks of metagabbros, amphibolites, charnockites and two pyroxene granulites of flesic as well as mafic associations (Fig. 1b). Minor amounts of feldspathoidal gneisses, granitoids, pegmatite veins and plagiogranite veins have also exposed. The detailed geology of the complex has been described by Yellappa *et al.* (2014) and Koizumi *et al.* (2014) and explained as Neoarchean to Paleoproterozic dismembered ophiolite complex. Based on the geochemistry of the mafic volcanics from the complex, it has been described as suprasubduction origin (Yellappa *et al.*, 2014).

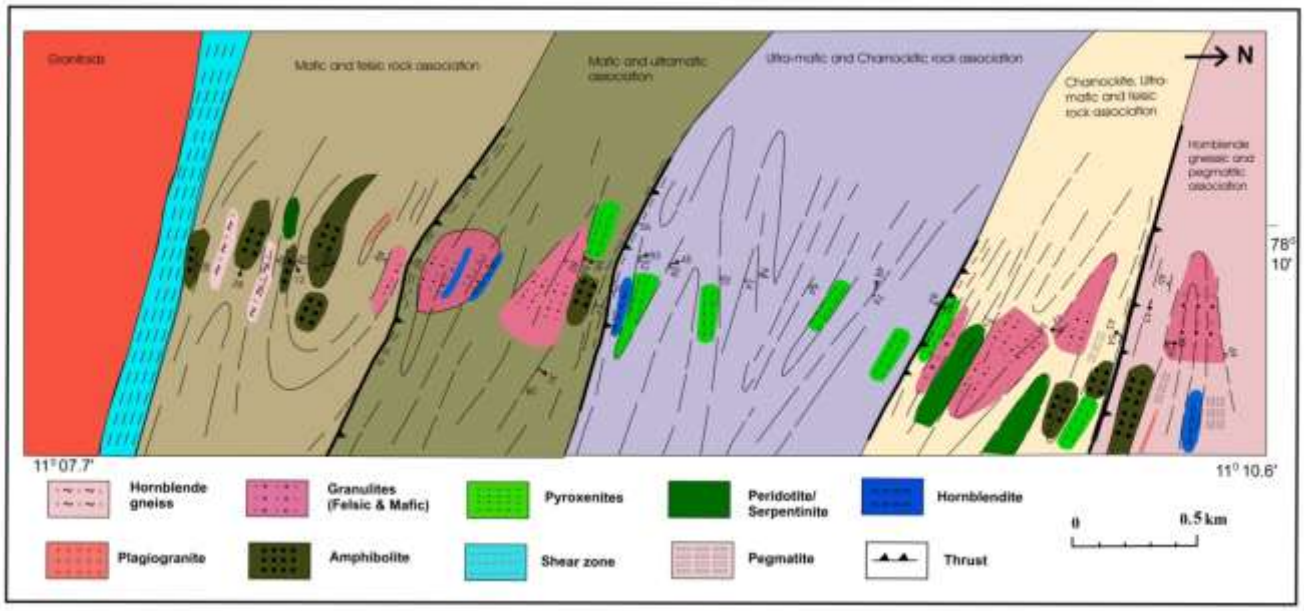

Fig. 2: Geological and structural map of AMUC (Namakkal-Mohanur Train cutting section) showing different lithological assemblages (after Yellappa et al., 2014).

The complex along train-cutting section has been described in to six zones based on distinct lithologial assemblages and the presence of important shear zones (Fig. 2; Yellappa *et al.*, 2014). Each zone is charecterized by the predominance of distinct lithological association and are classified as: Hornblende gneiss-Pegmatite association (Zone-I), Charnockite-Pegmatite association (Zone-II), Charnockite-Pyroxenite association (Zone-III), Granulite (Felsic and Mafic)-Amphibolite-Pyroxenite association (Zone-IV) and Metagabbro-Amphibolite-Pegmatite association (Zone-V). All the lithologies in general, highly sheared with intense mylonitization. The general strike of these rocks is WNW-ENE direction and dipping predominantly northwards with gentle to moderate angles. Some of the lithological contacts also show often steep dips ranging from 60^0-70^0. The rocks show regional isoclinal to tight fold structures with gentle plunges both in east and west, but dominantly to the east. At several places, the foliations preserve gentle (10^o-20^o) dips suggesting the early fold structures to be of recumbent nature. The deformation history and lithological contacts of several lithologies described by Yellappa et al. (2014). The mafic granulites have sharp contacts with ultramafic rocks (Fig. 3a) and exposed around 1.5 km strike length of thick horizon along the train-cutting section. The rocks show original metamorphic gneissic foliation and is mostly superimposed by subsequent mylonitic fabrics obscuring the early metamorphic gneissosity (Fig. 3b). Regionally, the two-pyroxene granulites represent marker horizons reflecting the isoclinal fold pattern in this region (Fg. 3c). The folds show varying thickness in the hinge regions and are highly stretched and extended in the high strain zones. However, the fold plunges remain same in the orientation but the plunge values are varying near the contacts. Presence of tectonic melanges is striking feature of the area. Some of the pyroxenites and hornblendites are also associated with mafic granulites in the form thin lenses, boudins and elongate veins (Fig. 3d and e). Another striking feature is occurrence of large porphyroclasts of garnets, mostly occur along the foliation planes surrounded by mafic material in the rims (Fig. 3f). These features are common in felsic granulates (Fig. 3g and h) also occurring adjacent to these lithlogies. Thin to thick quartzo felsdpathic veins have intruded parallel to the foliation planes (Fig. 3i). Intensely folded and deformed cherts and banded magnetite quartzites also occur in the form of thin horizons co-folded with two pyroxene granulites. Based on the field observations, it is described that a series of north dipping thrust/shear zones, associated with imbricate thrusts are linked to roof and floor thrusts suggesting that they could be of duplex structures emerging from the north (Yellappa *et al.*, 2014; Chetty *et al.*, 2016).

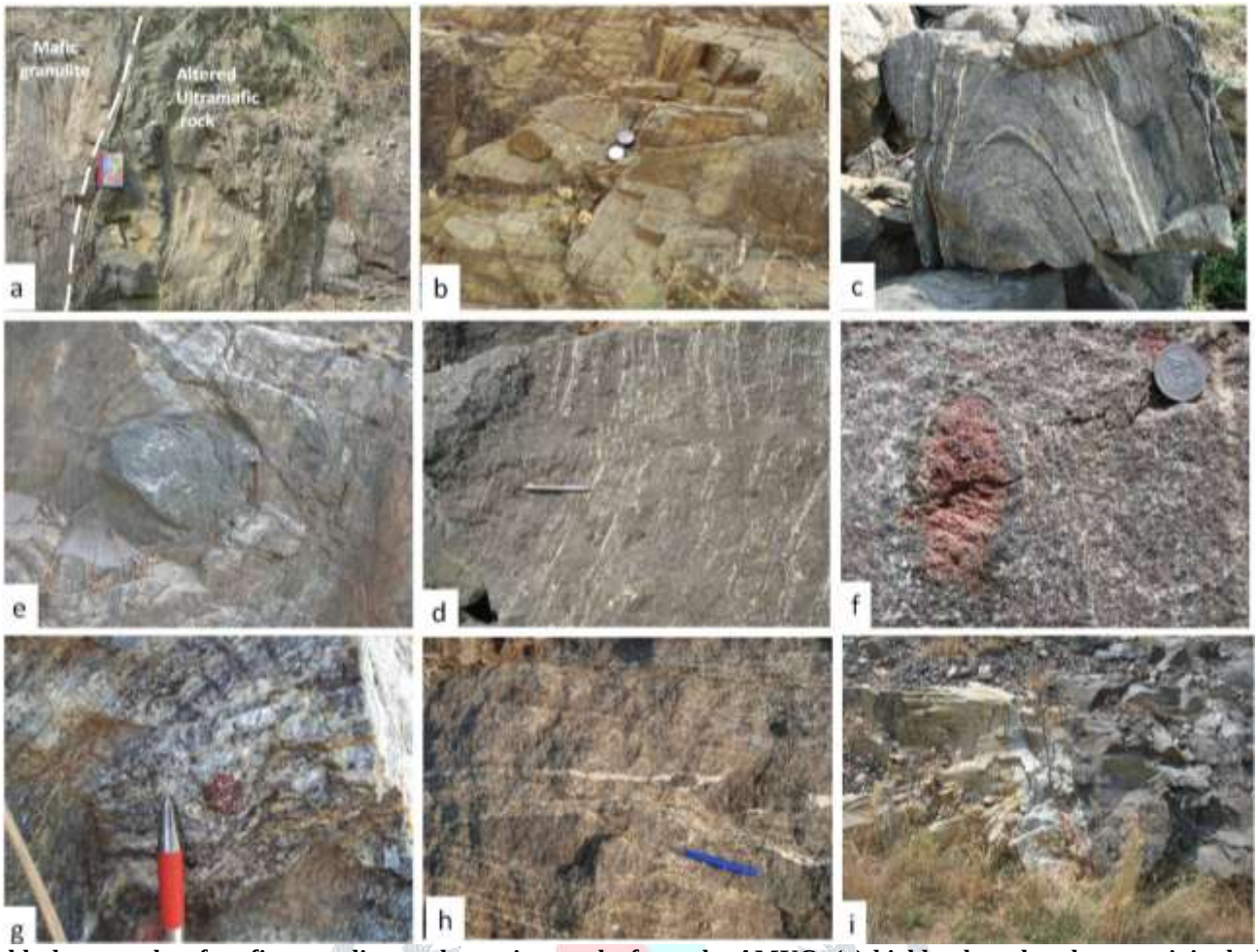

Fig. 3: Field photographs of mafic granulites and associate rocks form the AMUC: (a) highly altered and serpentinised ultramafic rock in contact with sharped contact of mafic granulite; (b) Deformed mafic granulites with primary metamorphic gneissic foliation; (c) & (d) outcrop scale isoclinal fold pattern in the granulites; (d) asymmetric large mafic boudin in deformed mafic granulite; (e) elongated thin hornblendite veins across the metamorphic foliation in mafic granulites; (f) large porphyroclasts of garnet with surrounded by mafic rim in mafic granulite; (g) outcrop of felsic granulite with garents; (h) eye shaped stretched asymmetric boudins in deformed felsic granulite; (i) intrusion of thick quartzo felsdpathic vein parallel to the foliation

4.2 Petrography

Mafic granulites are the second most abundant granulite-facies rock in the study area. Petrologically they having a gabbroic composition and display inequigranular granoblastic textures. Their mineral assemblages include plagioclase (5%) + biotite (1-2%) ± orthopyroxene (10-20%), ± clinopyroxene (40-50%) ± hornblende (10-20%) ± quartz ± garnet (20-30%). Zircon, titanite, apatite, allanite and opaque minerals are the common accessory minerals (0.1-0.5%) with secondary minerals like actinolite, cummingtonite, epidote and sericite. In most of the samples, the garnet occurs as porphyroblasts (Fig. 4a), especially when in contact with clinopyroxene, is partially replaced by fine-grained, radial and vermicular symplectites (Fig. 4b). Under the microscope the garnets show high relief, light pink in color (in PPL) with cubic-hexagonal shape and in some samples, it is a distinctive polygonal shape showing complete extinction. Many of the samples show several tiny fluid inclusions within the garnets, very similar to that in the matrix (Fig. 4c). Some of the garnets show two sets of cleavages (Fig. 5c). Clinopyroxene is subidioblastic is fine to coarse-grained (0.1-3 mm) and surrounded by fine-grained (up to 0.2 mm) idioblastic garnet. Exsolutions in Cpx are very common (Fig. 4d) and the lamella is highly deformed in some samples (Fig. 4e). In most of the samples, Cpx is altered in to amphibole. Orthopyroxene is also sub-idioblastic and fine- to coarse-grained (0.1-2.5 mm) with triple junctions. In some samples, Opx also show exsolutions and recrystallization of plagioclases along exsolution planes (Fig. 4f). Plagioclase is fine to coarse-grained (0.1-1.5 mm) with strong undulatory extinction and probable compositional zoning. It also occurs as commonly recrystallized form, optically continuous grains and symplectites around the garnets (Fig. 4a). Amphiboles occur as both, primary amphiboles which are dark green and fine to coarse-grained (up to 1.2 mm) with xenoblastic nature (Fig. 4a). Secondary amphiboles occur along the grain boundaries of Cpx and Opx that enclose all the peak minerals and also as symplectites together with some biotite flakes. Some of the amphiboles are mostly actinolites and fills the matrix of pyroxenes and garnet, it is regarded as a retrograde mineral (Fig. 4g). Rutile and opaque minerals occur together with amphiboles; therefore they could be also retrograde minerals. In some samples rutile and ilmenites occur adjacent to the amphibole, and they are sometimes exsolved from the amphibole. Zircon occurs either as intergranular grains or as inclusions in other minerals. Quartz is in marginal granulation as recrystallized and also occurs as symplectites around the garnets. Few samples of felsic granulites all also studied together, many of these show granitic textures and mainly composed of plagioclase (35-45%), quartz (35-45%), garnet (10-15%), clinopyroxene (5-10%), orthopyroxene (1-3%) with accessory minerals like amphibole, biotite, apatite, opaque mineral and zircon. The rocks are mostly deformed, most of the samples show mylonitic fabric with garnet rotated porrophyroblasts (Fig. 4h) and all minerals are stretched along the foliation of the rock. Plagioclase and quartz are dominant minerals and are fine to medium grained (~1.3mm). Garnets are subidioblastic and medium grained (0.2-0.5mm) and contains quartz and opaque minerals. Subidioblastic fine to medium grained (0.1-1.0mm), clinopyroxene and orthopyroxenes are also present. Amphiboles are mostly secondary occur around the garnet, clinopyroxene and orthopyroxenes. The quartz rich fluid inclusions occur within and around the garnets (Fig. 4i). These fluids are dominant in the felsic granulites compared to mafic ones.

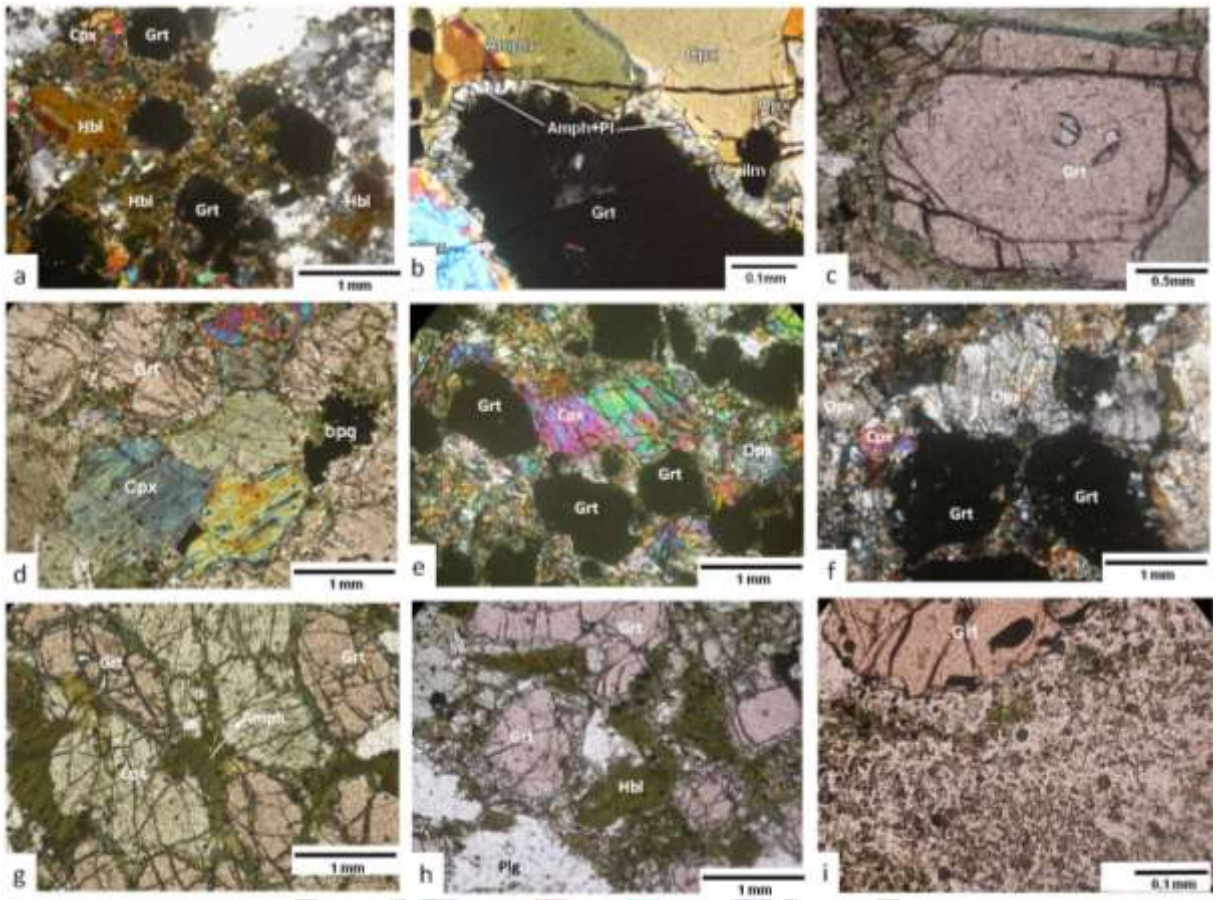

Fig. 4: Microphotographs of mafic and felsic granulites from the AMUC: ((a) euhedral garnet porphyroblasts with primary amphibole and pyroxenes; (b) partially replaced by fine-grained, radial and vermicular symplectites around garnet; (c) garnets show two sets of cleavages intersecting at 84^0 angle and presence of fluid inclusions; (d) presence of exsolution in Cpx lamella; (e) highly deformed Cpx lamella; (f) Opx show exsolutions and recrystallization of plagioclases along exsolution planes; (g) secondary amphibole crystallization around Cpx and garnet; (h) mylonitic fabric with asymmetric garnet porphyroclast in feslic granulite; (i) quartz rich hydrothermal fluids inclusions within and around the garnet of felsic granulite.

4.3 Geochemical characteristics

The mafic granulites relatively characterized by high SiO_2, varying from 37.94 to 52.87 wt.% and MgO from 4.57.6 to 12.16 wt.% with sample one of extremely high MgO 19.36 wt.%. The Mg number (Mg# =MgO/(MgO+FeO)) is between 0.273 and 0.557 for most of the samples but the higher ranges observed in the samples having higher Fe_2O_3 and TiO_2 contents. The Fe_2O_3 content is highly variable from 9.81 to 17.16 wt.%, increasing with increasing TiO_2 content (0.47-3.25wt.%.) These granulites show a rather narrow range in Al_2O_3 (10.13-115.89 wt.%) except one sample (7.95 wt.%) and CaO (8.86-15.36 wt.%). K_2O is also varies but relatively higher in some samples ranging 0.18-1.7 wt.% and P_2O_5 ranges from 0.02-0.64 wt,%. On the Harker geochemical diagrams (Fig. 5), CaO, Fe_2O_3 and SiO_2 are inversely correlated with MgO. Similarly, Fe_2O_3, TiO_2 and P_2O_5 also show a negative correlation with MgO (Fig. 6), which probably suggests a primary magmatic differentiation of the parental melt/igneous protoliths of these mafic granulites. Most of the oxides do not define any clear trends when plotted against MgO. However, Fe_2O_3 and TiO_2 are negatively correlated with MgO (Fig. 5), which suggests that the samples are not from a single magma or magmas, might have been intermingling or different episodes of origin. The Al_2O_3 and CaO show positive correlation with MgO respectively. The presence of higher concentration of Al_2O_3 results that possible occurrences of plagioclase in the liquidous phase and without garnet in the source mineralogy.

Table 1. Whole rock geochemistry of mafic granulites from the Aniyapuram Mafic Ultamfic Complex (AMUC)

Rock type			Mafic Granulite				
Sample no	ANP-51	ANPSS-2	AS-22	AS-22E	AS-22G	ANP-86A	ANP-87
SiO2	49.23	51.77	50.18	50.15	49.06	48.08	48.26
Al2O3	12.43	14.41	13.25	15.89	12.17	11.47	11.08
TiO2	1.3	1.17	1.09	0.91	2.28	0.88	0.47
Fe2O3	12.07	9.81	9.84	9.13	12.17	16.76	12.76
MnO	0.18	0.13	0.13	0.11	0.17	0.2	0.12
MgO	5.38	4.71	5.56	4.57	5.52	10.47	9.44
CaO	13.91	10.22	12.64	10.05	10.22	9.28	15.36
Na2O	3.68	6.1	4.8	7.27	4.99	1.32	0.47
K2O	0.36	0.35	0.36	0.3	1.73	0.26	0.13
P2O5	0.16	0.33	0.35	0.38	0.64	0.07	0.09
Sum%	98.7	99	98.2	98.76	98.95	98.79	98.18
Sc	36.524	24.74	32.98	27.79	44.8	9.854	13.699
V	220.033	198.2	235.7	181.2	399.3	295.778	435.995
Cr	344.202	185.1	130.7	265.4	98.67	2569.172	661.874
Co	50.248	115.5	124.2	107.4	152	90.008	67.136
Ni	84.655	142.4	132.6	226.9	125.2	551.61	196.794
Cu	52.326	71.23	66.98	109.2	112.9	21.2	91.115
Zn	81.393	90.07	101.6	146.2	173.4	185.217	278.536
Ga	4.646	7.786	8.388	9.561	17.45	21.494	26.175
Rb	0.388	0.216	0.376	0.078	20.58	3.99	1.412
Sr	52.648	438.3	322.8	696.8	554.7	92.942	57.056
Y	7.612	28.2	28.92	23.96	41.05	13.927	19.846
Zr	3.6	41.78	43.37	49.11	43.93	47.327	29.339
Nb	0.171	5.942	5.781	6.348	8.77	0.143	0.046
Cs	0.019	0.002	0.023	0.004	0.075	0.05	0.06
Ba	19.843	104.4	170.9	172.7	829.6	64.04	43.007
Hf	0.2	4.001	7.234	3.632	2.999	1.113	0.869
Ta	0.018	0.876	0.715	0.616	0.759	0.013	0.028
Pb	3.186	0.472	0.808	1.659	4.274	4.084	5.683
Th	0.021	0.024	0.053	0.05	0.403	0.05	0.056
U	0.004	0.01	0.029	0.013	0.177	0.092	0.126
La	10.55	11.62	12.17	14.52	26.12	2.484	1.975
Ce	10.543	25.95	27.6	29.79	49.76	8.48	7.716
Pr	0.284	4.172	4.366	4.592	7.079	1.337	1.401
Nd	1.693	19.32	20.64	22.14	32.8	7.882	8.664
Sm	0.687	4.753	4.997	5.344	8.173	1.933	2.283
Eu	0.424	1.485	1.356	1.868	2.585	0.644	0.718
Gd	1.089	2.95	2.88	3.029	4.807	2.651	3.064
Tb	0.224	0.82	0.731	0.72	1.115	0.412	0.505
Dy	1.354	5.52	4.882	4.438	6.759	2.503	3.11
Ho	0.303	1.074	1.018	0.884	1.341	0.476	0.663
Er	0.775	2.389	2.487	2.033	3.362	1.444	2.149
Tm	0.113	0.425	0.465	0.363	0.647	0.194	0.325
Yb	0.561	2.868	3.031	2.274	4.009	1.259	2.189
Lu	0.075	0.486	0.484	0.347	0.588	0.152	0.289
REE total	28.675	83.832	87.107	92.342	149.145	31.851	35.051
Mg#	30.8309456	32.4380165	36.1038961	33.3576642	31.2040701	38.4502387	42.5225225
K/Rb	7699.87595	13447.057	7945.61667	31918.2892	697.611588	540.771015	764.049698
Ba/La	1.88085308	8.98450947	14.042728	11.8939394	31.7611026	25.7809984	21.7756962
La/Yb_N	13.0439565	2.81026143	2.78499477	4.42890024	4.51915106	1.36850253	0.62580796
Sm/Nd_N	1.24773075	0.75645273	0.74442467	0.74218117	0.76617637	0.75407844	0.81023046
Ce/Yb_N	5.0800927	2.44584261	2.46146371	3.54119902	3.3551706	1.82070848	0.95283291
La/Sm_N	9.60605779	1.52928274	1.52345876	1.69961142	1.9991305	0.80383925	0.54114128
Gd/Yb_N	1.60615109	0.85106797	0.78619075	1.10212332	0.99210913	1.74222955	1.15814884

Table. 1 contnd…

		Mafic Granulite					
Sample no	ANP-87A	ANPSS-16	ANPSS4	ANP 11	ANP-22H	ANP-80	ANP-13
SiO2	37.94	47.23	49.19	48.52	50.32	52.87	49.24
Al2O3	10.13	12.13	7.95	11.22	11.21	13.89	13.81
TiO2	0.59	1.52	2.2	1.05	3.25	0.51	1.54
Fe2O3	15.34	13.48	12.76	17.16	13.95	11.52	14.31
MnO	0.15	0.17	0.2	0.18	0.3	0.1	0.13
MgO	19.36	7.34	12.16	7.26	5.25	7.75	6.2
CaO	14.23	11.34	12.19	11.22	10.93	8.86	10.73
Na2O	0.96	4.01	2.03	1.31	2.54	2.59	1.95
K2O	0.1	0.5	0.12	0.26	0.01	0.18	0.29
P2O5	0.13	0.56	0.02	0.22	0.63	0.11	0.45
Sum%	98.93	98.28	98.82	98.4	98.39	98.38	98.65
Sc	5.926	46.44	13.34	27.4	64.3	8.6136	43.896
V	141.894	368.8	92.92	224.959	172.6	64.1122	502.158
Cr	1741.842	112.7	155.76	332.512	68.96	126.359	380.319
Co	89.801	165.9	35	44.655	200.6	11.019	66.511
Ni	113.703	74.01	79.86	109.378	10.49	81.8666	66.57
Cu	75.188	158.9	6.418	34.246	470.7	6.1576	48.435
Zn	223.255	146.2	40.9	81.928	193.3	15.498	129.779
Ga	12.051	12.57	1.8988	14.609	9.341	9.6352	37.172
Rb	2.729	0.455	5.097	2.948	0.088	2.8082	7.143
Sr	68.375	1293	38.39	115.778	102.4	71.927	840.845
Y	7.736	40.38	18.242	21.351	116.6	10.1886	38.851
Zr	34.42	58.41	127	80.371	60.54	9.998	38.12386
Nb	0.146	6.42	4.118	2.474	14.2	1.565	3.3494
Cs	0.539	0.018	0.001	0.769	0.003	0.4704	0.346
Ba	48.436	246.9	31.6	74.404	47.91	47.7218	314.84
Hf	0.944	3.512	3.72	2.153	4.772	4.312	4.7839
Ta	0.014	0.735	1.033	0.381	1.808	0.3818	0.864
Pb	10.029	6.02	0.377	3.395	4.7213	2.9094	1.664
Th	0.415	0.136	0.758	1.92	0.02	2.7122	0.92
U	0.269	0.055	0.2676	1.396	0.027	1.7186	0.652
La	3.802	22.15	3.11	12.795	10.2	9.934	7.253
Ce	8.793	47.54	10.35	32.214	28.53	19.5904	16.5278
Pr	1.19	7.901	2.056	4.178	5.494	2.2014	2.0664
Nd	6.027	37.75	11.326	22.065	31.75	9.9158	10.7868
Sm	1.139	9.116	3.644	5.006	11.42	1.9236	2.2844
Eu	0.31	2.559	0.4846	1.232	2.794	0.5156	0.6246
Gd	1.502	5.407	2.004	4.288	7.756	1.739	1.974
Tb	0.218	1.179	0.5062	0.569	2.555	0.2342	0.2368
Dy	1.258	6.863	3.16	3.59	19.07	1.5576	1.3886
Ho	0.271	1.318	0.626	0.693	4.196	0.3266	0.2536
Er	0.801	3.138	1.4602	1.941	10.25	0.9706	0.6902
Tm	0.117	0.536	0.2522	0.234	2.033	0.125	0.0786
Yb	0.781	3.132	1.4664	1.53	13.02	0.8708	0.5102
Lu	0.099	0.48	0.209	0.32	2.1	0.193	0.1044
REE total	26.308	149.069	40.6546	90.655	151.168	50.0976	44.7794
Mg#	55.7925072	35.2545629	48.7961477	29.7297297	27.34375	40.2179554	30.2291565
K/Rb	304.095097	9119.51119	195.379757	731.911923	943.040362	531.933599	336.922722
Ba/La	12.7396107	11.1467269	10.1607717	5.81508402	4.69705882	4.80388565	43.4082449
La/Yb_N	3.37660937	4.90536942	1.47105083	5.80054234	0.54338661	7.91271416	9.86045522
Sm/Nd_N	0.58109031	0.74252052	0.98928839	0.69760248	1.10597033	0.59649679	0.65117936
Ce/Yb_N	3.04338105	4.10305857	1.90791134	5.69145774	0.59232639	6.08128246	8.75678903
La/Sm_N	2.08803542	1.51991355	0.53386505	1.59881759	0.55870626	3.23041903	1.98607204
Gd/Yb_N	1.59125682	1.42842024	1.13075012	2.31891444	0.49288794	1.65235188	3.20131251

The trace elements concentration are varying for many samples, the Ni and Cr range from 67 to 227 ppm (except one sample of higher concentration 551.6 ppm) and from 98.67 to 380 ppm, respectively. However three samples show slightly higher concentrations of 663, 1743 and 2569 ppm. The incompatible trace elements such as Nb, Ta, Zr, Hf are relatively low abundances, which confirm the sub-

alkaline nature of their lower crustal protoliths. Rb abundances are very low (0.1-7.2 ppm except one sample of 21ppm) and giving higher K/Rb ratios of 195-13447 (one sample shows 31918). Ba contents are relatively variable range from 20 to 830 ppm.

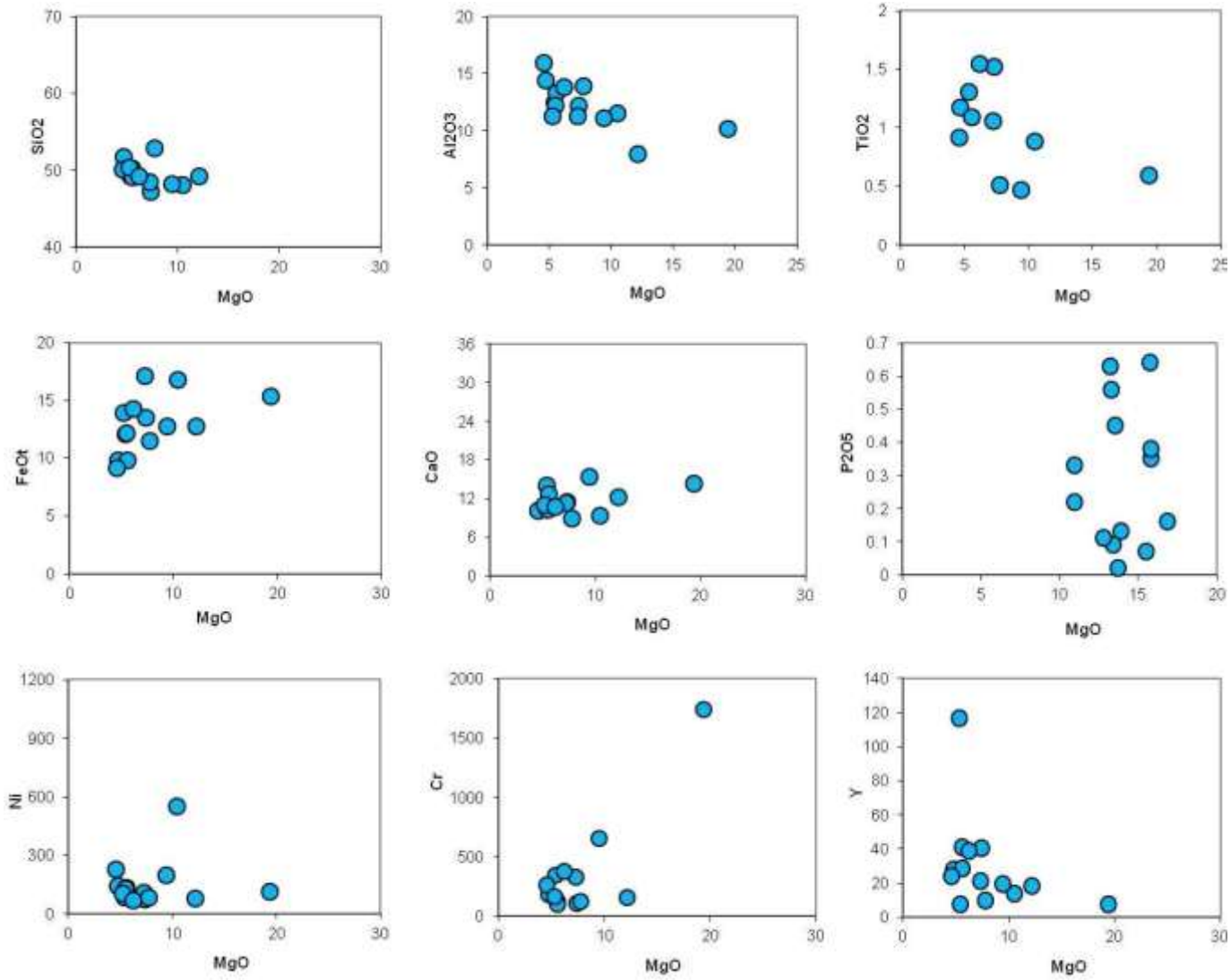

Fig. 5: Geochemical binary plots for mafic granulites: MgO (wt%) vs. SiO_2 (wt%); MgO (wt%) vs. TiO_2 (wt%); MgO (wt%) vs. Al_2O_3 (wt%); MgO (wt%) vs. FeO(t) (wt%); MgO (wt%) vs. CaO (wt%); MgO (wt%) vs. Ni (ppm); MgO (wt%) vs. Cr (ppm); MgO (wt%) vs. Y (ppm)

On the Zr/Ti vs. Nb/Y classification diagram (Winchester and Floyd, 1977), all these mafic granulite samples plot in the sub-alkaline basalt to basaltic andesite fields (Fig. 6a). In ternary plot (Al-(Fe^t+Ti)-Mg) of Jensen (1976), these samples dominantly plotted in Mg to Fe tholeiite basaltic field and few plotted in komatiitic basaltic field (Fig. 6b) and on triangular geochemical A-F-M diagram (Na_2O+ K_2O-FeO^t-MgO, Fig. 6c; Irvine and Baragar, 1971) many samples were plotted in tholeiitic field. Similarly, on binary diagram of Zr vs. Y ppm (Fig. 6d), these rocks dominantly exhibit a tholeiitic character.

The mafic granulites of AMUC have high REE contents ranges from 26.4 to 151.2 ppm. The LREE's are higher in concentration than HREE. Chondrite-normalized REE ratios of $(La/Sm)_N$, $(La/Yb)_N$ and $(Gd/Yb)_N$ range from 0.54 to 2.11 (except one sample of 9.60) and 0.63 to 9.86 (one sample show higher ratio of 13.04) and from 0.49 to 3.208 respectively. All the samples represent almost a flat REE trend (Fig. 7a) may represent derivation from nearly non enriched sources by higher degrees of partial melting with light fractionation of mafic phases. Another the feature of these samples show both positive and negative europium anomalies with Eu/Eu_N* ratio of 1.41 to 5.16, which probably indicates lesser plagioclase accumulation in the parental melt. On N-MORB normalized spider plots, the large ion lithophile elements (LILE: Rb, Ba, K, La, Ce, and Sr) do not show a smooth pattern. The plots show enrichment of LILE, except for three samples which show depletion of K and Rb with negative anomaly of Sr and Th (Fig. 7b). This prominent enrichment anomaly of LIL probably suggests a crustal influence. The high field strength elements (HFSE: Nb, Sm, Nd, P, Zr, Ti, Y and Yb) show depleted pattern although Nb shows a negative anomaly in many samples and Ti has prominent negative as well as positive anomaly in few samples.

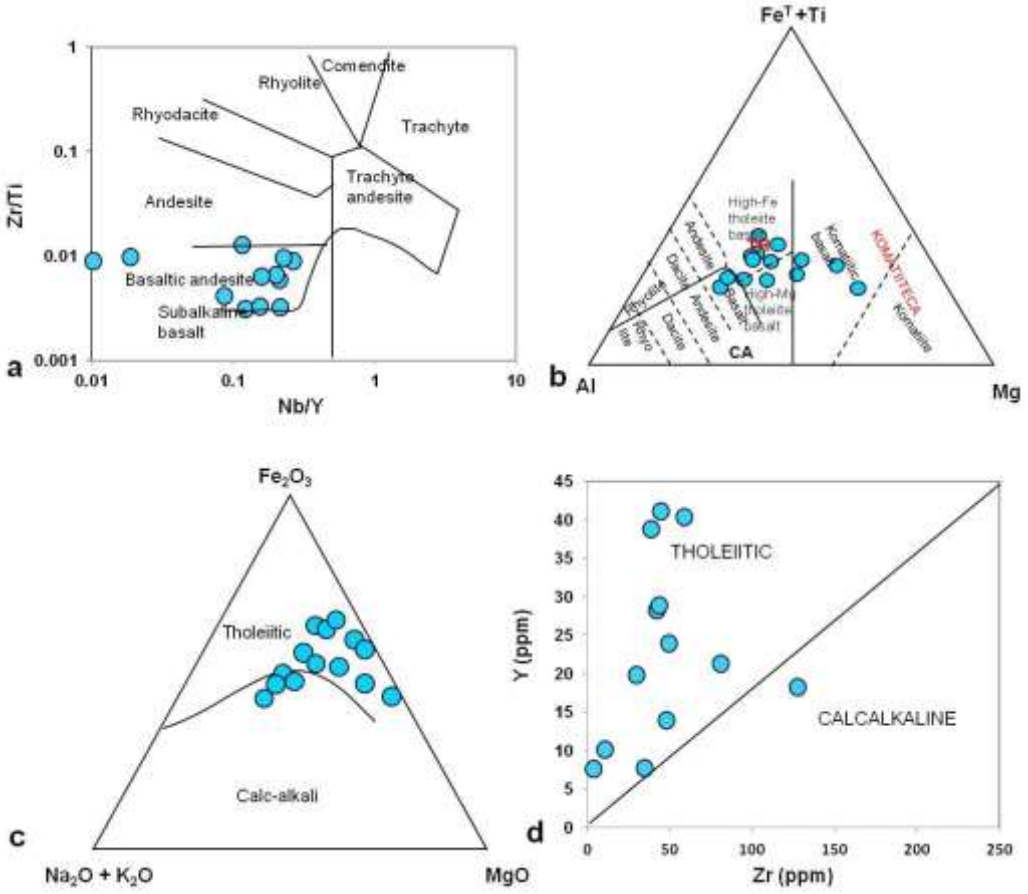

Fig. 6: Geochemical variation plots for mafic granulites: (b) Zr/Ti vs. Nb/Y diagram (after Winchester, and Floyd,1977); (b) ternary plot of Al-(Fe^t+Ti)-Mg (after Jensen, 1976); (c) Fe_2O_3-Na_2O+K_2O-MgO geochemical variation diagram of mafic granulites (after Irvine and Baragar, 1971); (d) Y (ppm) vs. Zr (ppm) diagram classification diagram (after Barrett and Mac Lean, 1994)

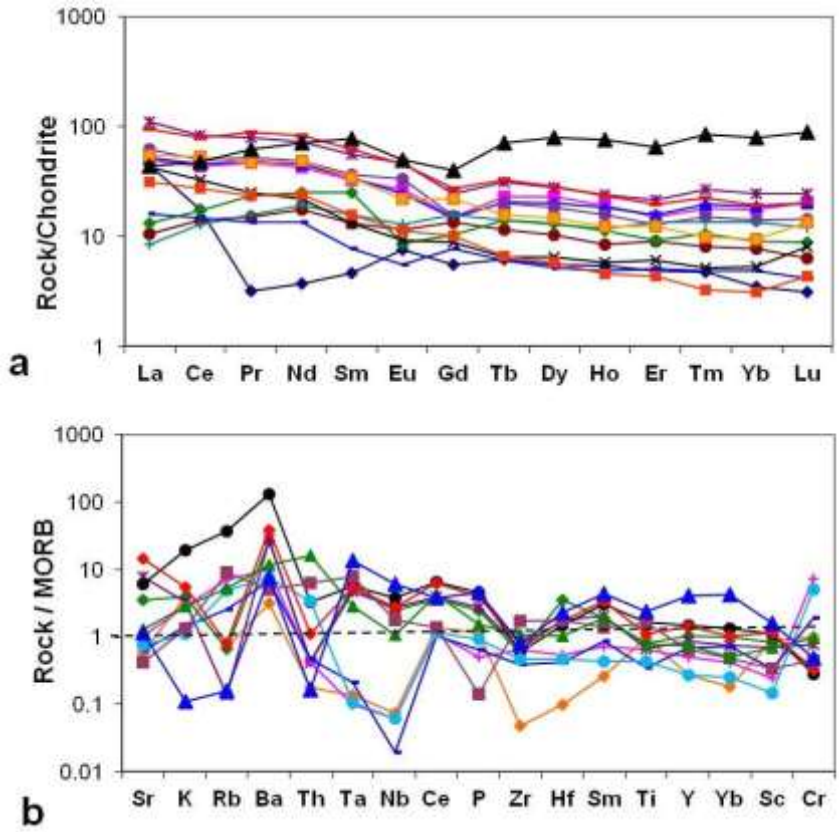

Fig. 7: Spider plots for mafic granulites: (a) Chondrite normalized diagram (after Sun and Mac Donough, 1989); (b) MORB normalized incompatible element diagram (after Sun and Mac Donough, 1989).

5 DISCUSSION

The aim of this study is to present new comprehensive geochemical data, together with petrographical and field observations in order to put constraints on the genesis and evolution history of mafic granulites around Aniyapuram in the central part of CSZ. Petrological studies revealed that, the mafic granulite are granoblastic textures of high-grade metamorphics with symplectites, coronas around garnets and exsolution textures in clinopyroxenes and triple junctions of orthopyroxene suggesting varied metamorphic gradient. Field observations suggest that the granulites have undergone large-scale deformation with mylonitic fabric and stretched phenocrysts, prophyrobalsts of mafic assemblages showing compositional variations from mafic to felsic assemblages on different scales.

5.1 Protolith of Mafic Granulites

The geochemical data from the mafic granulites of the Aniyapuram reveals the majority of the samples display tholeiitic nature (Fig. 6a and b) with strong iron enrichment similar to basaltic nature of volcanic origin. It is well described that two pyroxene granulites found in many volcanic ejections and consider as magmatic origin if its basaltic melt or metamorphic origin based on the mineral assemblages (Kay and Kay, 1983). Majority of the samples are inversely correlated with major oxides especially SiO_2, Fe_2O_3 TiO_2 and P_2O_5 and trace Ni and Y against MgO suggest a primary magmatic differentiation of the parental melt/igneous protoliths. Such characteristic features of mafic granulites and charnockites were described in several parts of the terrain (Weaver, 1980; Moses *et al.*, 1999; Tomson *et al.*, 2006, 2013). The geochemical classification diagrams of these mafic granulites show tholeiitic affinity (Fig. 6b-d) and LREE enriched on chondrite-normalised pattern with distinct Eu +ve anomaly (except few samples) implying plagioclase fractionation. Similar characteristics of mafic granulites of Kanjamalai have been reported (Bose *et al.*, 2001). The geochemical data is also plotted on various tectonic discrimination diagrams, which are typically used for distinguishing Mid Oceanic Ridge Basalt (MORB) and Island Arc Tholeiite (IAT). It is well described that the minor and trace elements must be relatively immobile during granulite facies metamorphism and metasomatism (Shu *et al.*, 2004). In the TiO_2-MnO-P_2O_5 ternary tectonic diagram (Fig. 8a), some samples plot in Island arc tholeiite field, and some other samples plot in Ocean Island Arc (OIA) field (Mullen, 1983). In Ti vs. Zr tectonic discrimination plot (Fig. 8b; Pearce, 1980) many samples show arc signature except three samples, plot in MORB fields. Similarly in V vs. Ti/1000 plot (Fig. 8c, Shervais, 1982), many samples dominantly plot in arc field with intersection of MORB field and Ocean Floor Basaltic fields (OFB, two samples).

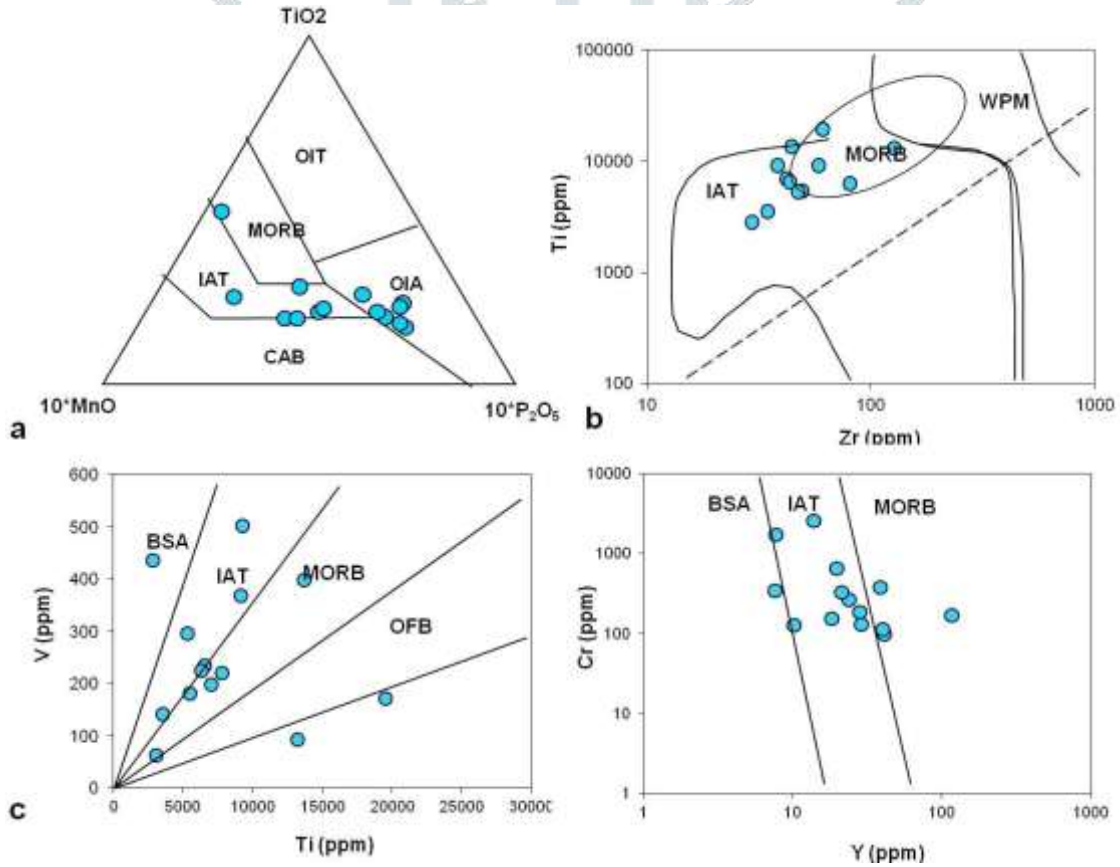

Fig. 8. Geochemical tectonic discrimination plots for mafic granulites (a) TiO_2-MnO-P_2O_5 ternary diagram (after Mullen, 1983); (b) Ti (ppm) vs. Zr (ppm) discrimination diagram (after Pearce, 1980) (c) V (ppm) vs. Ti (ppm) discrimination diagram after (after Shervais, 1982); (d) Cr (ppm) vs. Y (ppm) discrimination diagram (after Pearce, 1982); IAT: Island Arc Tholeiite, MORB: Mid Ocean Ridge Basalt, WPB: Within-Plate-Basalt; OFC: Ocean Floor Calc-alkalis, OIA: Ocean Island Alkali-basalt, CAB: Calc Alkali Basalt.

In Cr vs. Y (Fig. 8d) many samples show major IAT source (Pearce, 1982) and few overlap with MORB. On spider plot with normalized MORB (Fig. 7b), these mafic granulites show LILE (K, Rb, Ba, Th) enrichment and HFSE (Ti, Nb, Hf,) depletion with negative Nb anomalies clearly represent suprasubduction zone (SSZ) tectonics of origin. All these geochemical signatures are similar to mafic volcanics of this complex described by Yellappa et al. (2014). This implies that the protolith of these granulites might be a upper part of ophiolite sequence/ mafic volcanics as well as gabbroic intrusions of tholeiitic nature developed under suprasubduction setting. The subduction related origin of high-grade rocks were described by several workers in the terrain; the geochemical characters of the charnockitic massifs in the Madurai Block described as strong calc-alkaline affinity (Chacko *et al.*,1992-Cardamom Hill Charnockites; Tomson *et al.*, 2006) and the charnockites of the Cardamom Hills also described as subduction related origin (Rajesh, 2007, 2012). The mafic granulites AMUC have higher silica content but are lower in MgO and slightly lower CaO and show wide variation in Rb concentration (0.03-20.58 ppm). The Rb

content in these granulites is much lower than those of the average crustal rocks (Rudnick and Gao, 2003). The higher K/Rb values (up to 31918) with K-contents lower than 1 wt.%, is observed in these granulites. These higher K/Rb ratios are mainly due to break down of biotite to orthopyroxene, alkali feldspar and melt under granulite facies condition and escape of the melt from the system (Rudnick *et al.,* 1985). Similar geochemical characteristic features of mafic granulites were reported in the western part of CSZ (Prakash *et al.,* 2012) and from many granulitic terrains of the world (K/Rb values, Sheraton and Collerson, 1984).

5.2. Metamorphism and Age Constraints

The garnet-bearing high-grade assemblages from SGT has been distinguished in to high pressure granulites (P = 8.3 ± 1.0 kbar; T = 760 ± 40°C) including the charnockites and mafic granulites in northern slopes of the Nilgiris; medium pressure granulites (P = 6.4 ± 1.0 kbar; T = 735 ± 40°C) includes the charnockites of the central Nilgiris and the Madras granulites to the east and low pressure granulites (P = 5.0 ± 1.0 kbar; T = 700 ± 20°C) of charnockites and metapelites to the south of Bhavani shear zone (Hariss *et al.,* 1982). The geochemical data of AMUC mafic granulites together with mineral composition data (Kouzumi *et al.,* 2014) reveal that the protolith is calc-alkaline basaltic in nature and granulite facies metamorphism taken place at peak P-T conditions of 9.8-10.6 kbar and 730-790^{0}C, followed by decompression to 6.5-8.0 kbar and ca. 750^{0}C. It was also recorded the extreme crustal metamorphism at T = 900-1150^{0}C and P = 7-13 kbar in some parts of SGT, which are generally designated as ultra-high temperature (UHT) metamorphic rocks (Harley, 2004). The P-T conditions of metamorphism of the Kanjamalai mafic granulites in northern part of CSZ has described similar P-T conditions of 900 ± 59^{0}C and 14 ± 2 kbar (Mukhopadhyay and Bose, 1994). In the AKSZ of Trivandrum block it is described that the P-T estimates up to 8.5-9 kbar and 940-1040°C from cordierite and orthopyroxene-bearing ultra high temperature (UHT) granulites (Ishii *et al.,* 2006). Some studies (Braun *et al.,* 1996; Nandakumar and Harley, 2000; Cenki *et al.,* 2004) have also explained that the P-T estimation from KKB represents the highest-grade assemblages record temperatures of 840^0-1070^{0}C and pressures up to 9.5 kbar. The metapelite rafts within enclosed the charnockites in southern-most tip of peninsular India in the Nagercoil Block inferred the peak metamorphic pressures of 6-8 kbar and temperatures in excess of 900^{0}C (Johnson *et al.,* 2015). All these tectono metamorphic events are coeval with the granulites of AMUC. The P/T fields of several high-grade assemblages within the terrain are consistent with metamorphism induced by a CO_2-rich vapour phase rising from the mantle (Harris *et al.,* 1982). The AMUC mafic granulites are associated with dismembered ophiolite sequence, charncokites, felsic assemblages etc. The petrography shows occurrence of several fluid inclusions within these granulites especially in the garnets associated with quartz and apatites. These fluids are probably CO_2 rich and might be expelled from the deeper levels during high-grade metamorphism (Newton *et al.,* 1980; Frost and Frost, 1987; Santosh and Omori, 2008; Toruet *et al.,* 2016), related to Neoproterozoic arc magmatism (Santosh *et al.,* 2009; Teale *et al.,* 2011; Kouzumi *et al.,* 2014) in the terrain/CSZ. It is also well described that the occurrence of abundant CO_2 rich inclusions in Mg-Al-rich mafic granulites and retrogressed eclogites (high-pressure granulites) and in some of the metamorphic rocks of the CSZ (Sikantappa *et al.,*1992; Santosh *et al.,* 2003; Nishimiya *et al.,* 2008). In some other study, from the UHT terrains of the Trivandrum and Madurai Blocks reported the occurrence of primary fluid inclusions with markedly low-density CO_2 (Tsunogae *et al.,* 2008).

The U-Pb ages of zircons from the metagabbros of this complex is reported the Paleoproterozoic age of ca 2436 ± 22 Ma magmatic emplacement of the protolith and Cryogenian (ca 731 ± 11 Ma) thermal event or high-grade metamorphism (Koizumi *et al.,* 2014). The Neoproterozoic metamorphic ages are coeval to the magmatic emplacement ages of Manamedu ophiolite complex (Santosh *et al.,* 2012) and Kadvur anorthositic gabbros (Teale *et al.,* 2011). Similar ages of Neoproterozoic granulite metamorphism in the terrain were also described by several workers in the south of CSZ within the terrain (Santosh *et al.,* 2003; Ghosh *et al.,* 2004; Bhutani, *et al.,* 2007; Brandt *et al.,* 2011). Recently, several Neoproterozoic ages of the high-grade assemblages were also reported from the south of CSZ (Brandt *et al.,* 2014; Plavsa *et al.,* 2012, 2014).

Among these, the Mesoarchean granulite metamorphism was also described by many workers in the north west of CSZ (Choudhary *et al.,* 2011; Amaldev *et al.,* 2016). The Neoarchean (ca. 2.7-2.5 Ga) to early Paleoproterozoic (ca. 2.5-2.48 Ga) granulite facies metamorphism also has been described in different blocks of the terrain by several workers (Raith *et al.,* 1999; Ghosh *et al.,* 2004; Anderson *et al.,* 2012; Brandt *et al.,* 2014; Glorie *et al.,* 2014). The protoliths of the Salem Block described that Meso- to Neoarchean rocks stretching as far south as the CSZ with metamorphic age's and has been reported that the granulite facies event in the latest Archean to earliest Proterozoic (Peucat *et al.,*1993). The early Paleoproterozoic (ca. 2490 Ma) metamorphic ages with pressure-temperature (*P-T*) conditions of ~14-16 kbar, ~820-860 °C were described from Kanja Malai Hills of the Salem block (Saitoh *et al.,* 2011; Anderson et al., 2012). It is also described that the ages and metamorphism of Nilgiri highland massif for the garnetiferous enderbites and granulites as 2460±81; Ma 2506±70 Ma respectively, based on the Rb-Sr and Sm-Nd evolution studies (Raith *et al.,* 1999). In another study, the Nilgiri block was metamorphosed under medium-high pressure granulite facies conditions (6-10 kbar; Harris *et al.,* 1994). In the Madurai Block of northern part, it is described that the emplacement age and magmatic protolith of migmatitic garnet-orothopyroxene gneiss as 2493 ± 10 Ma and granulite-facies metamorphic event proposed as 2472 ± 15 Ma (Brandt et al., 2014.). The timing of protolith formation for sapphirine-bearing granulites and garnet-cordierite gneisses from the NW of Madurai, described as 2509±12 Ma and 2509±30 Ma based on U-Pb zircon ages (Prakash, 2010). The metamorphism along Kerala Khondalite Block (KKB) described as a clockwise P-T path with post peak isobaric cooling followed by isothermal decompression (Cenki *et al.,* 2004). All these ages are coeval with emplacement age of AMUC protoliths.

5.3. Tectonic Implications

Geochemical data of AMUC, particularly REE and some trace elements (negative Nb, Zr, P Ti anomalies and LIL enrichment), together with available age data (ca. 2436 ±32 Ma; Koizumi *et al.,* 2014) suggest the protolith origin of these granulites related to similar to the origin of mafic volcanics (Island arc) of the complex (Yellappa *et al.,* 2014) during Neoarchean to Paleoproterozoic suprasubduction zone mechanism. Such Neoarchean suprasubduction tectonics within the CSZ has been described by several workers (Yellappa *et al.,* 2012; Noack *et al.,* 2013; Santosh *et al.,* 2013). The occurrence of Devanur Ophiolite Complex (DOC), Agali Ophiolite Complex (AOC), Neoarchean Oceanic crust related sequence with BIF association at Kanjamalai Complex (Noack *et al.,* 2013) and Sittampundi Anorthosite Complex (Dutta *et al.,* 2011) are few examples of evidences. Similar Neoarchean arc magmatism and subduction related evidences described in several parts of the terrain: the geochemistry of the amphibolites, metagabbros, charnockites and TTG gneisses around Nilambur area in western part of CSZ, described as subduction-related intra-oceanic tholeiitic arc basalts developed in Neoarchean primitive arc magmatic settings with MORB-like components (Shaji *et al.,* 2014). In the northern part of CSZ, the evolution of Biligiri Rangan Hill granulites and its protoliths described as partial melting of young hydrated oceanic crust in a subduction zone-like environment based on geochemical and isotopic ratio (Janardhan *et al.,* 1994). The Neoarchean subduction-accretionary tectonics and 2650 Ma and 2490 Ma metamorphism of charnockites, pink granite and mafic granulites described from Biligiri Rangan Block (Ratheesh Kumar *et al.,* 2016). The occurrence of arc-

related volcano magmatic suite along the northern periphery of Nilgiri Block described as a prominent Neoarchean arc magmatism and early Paleoproterozoic convergent margin processes in the terrain (Samuel *et al.,* 2014). It is also well documented the arc-arc and arc-continental accretion, tholeiitic as well as komatiitic ultramafic and mafic volcanism and followed by major juxtaposition of continental arc assemblages to the southern margin of the Dharwar craton during the Neoarchean period (Praveen *et al.,* 2013). The evolution of orthongneisses and high-grade rocks include felsic granulites-charnockites in Keral Khodalite Belt also described the subduction related magmatism followed by arc accretion (Ravindrakumar and Sreejith, 2016).

The formation of the granulites has been broadly described under two tectonic environments: (i) Continent-continent collision in which the lower plate in the subduction process is buried to great depth and heated through thermal relaxation results and granulite-eclogite facies metamorphism and (ii) Magmatic arc setting, under and intra-plated mantle derived basaltic magmas followed by granulite facies metamorphism, partial melting of country rocks with development of granitoids and charnockitic magmas (Percival, 1994). The Cauvery Suture Zone in the terrain is well described as a complex zone of multiple ocean closure followed by seduction-collison-acretionary processes and intrusions of charnockitic magmas and felsic volacanism both in the Neoarchean as well as in Neoproterozoic (Ghosh *et al.,* 2004; Santosh *et al.,* 2012; Yellappa *et al.,* 2012; Collins *et al.,* 2014). It is also interpreted that the CSZ as zone of closure of the Neoproterozoic Mozambique Ocean (Santosh *et al.,* 2009; Collins *et al.,* 2007) is thought to have occurred during the late Neoproterozoic at the end of Precambrian along with the formation of Gondwana. The granulite metamorphism of metagabbros of this complex described the Neoproterozoic age of 731±11Ma (Koizumi *et al.,* 2014). The magmatic ages of the plagiogranites and gabbros of Manamedu Ophiolite Complex within the CSZ yielded the similar ages of 737 ± 23 to 782 ± 24 Ma; 744 ± 11 to 786 ± 7.1 Ma (Santosh *et al.,* 2012). The Kadavur gabbro-anorthosite and Rapakavi granite from the CSZ show the ages of 825 ± 17 and Ma 819 ± 26 Ma (Sato *et al.,* 2011; Teale *et al.,* 2011). Based on the U-Pb ages of zircons and geochemistry of Angadimogar syenite (781.8 ± 3.8 Ma to 798 ± 3.6 Ma) and Peralimala alkali granite (797.5 ± 3.7 Ma and 799 ± 6.2 Ma) in north western margin of the terrain represent Cryogenian alkaline magmatism (Santosh *et al.,* 2014, 2017). All these corresponding evidences suggest a prominent mid Cryogenian arc magmatism-followed by subduction accretion system along the southern margin of the CSZ, results the production of enormous heat and hydrothermal CO_2 rich fluids have been responsible for the occurrence of higher amphibolites-granulite facies metamorphism of these rocks. The above studies with reference to of ophiolite emplacement it is observed that the formation and evolution of these granulites might taken place probably in two intervals; in the early stage of oceanic crustal subduction, origin of calc-alkaline basalt within island-arc environment followed by collision, ophiolite emplacement during Neoarchean and in later stage, the occurrence of granulite facies metamorphism in association with Neoproterozoic arc magmatism.

6 CONCLUSIONS

1. Field characteristics and petrological studies of mafic granulites in association with mafic-ultramafic rocks suggest that the development of Grnt-Cpx-Hb-Pl assemblages might be connected with ophiolite emplacement and subduction /collision.
2. The geochemistry of these mafic granulites indicate that the protoliths are calc alkaline to tholeiitic basalts which were probably formed in suprasubduction zone tectonic setting related to Neoarchean to Paleoproterozoic dismembered ophiolite sequence of the region.
3. Enrichment of LILE (Sr, K, Rb, Ba) and depletion of HFSE (Ti, Nb, Ta, Hf) with N-MORB and depletion of Nb in mafic
4. granulites reflects the source characteristic confirming an Island arc environment of their original magma formation.
5. The evolution of these granulites might have been undergone in to two episodes: the initial period includes crustal subduction, origin of thoeliitic to calc-alkaline magmas in island-arc environment during Neoarchean-Paleoproterozoic time and underwent granulite facies metamorphism during Middle to Late-Neoproterozoic periods in association with arc magmatism.

ACKNOWLEDGEMENTS

The author is thankful to the Director, CSIR-NGRI, Hyderabad for the encouragement, support and permission to publish this article. We are also thankful to our colleagues Dr. Venkatasivappa, Dr. A. Keshava Krishna and Mr. S. Balu for their help in geochemical analysis. This work forms a part of Department of Science and Technology, Government of India, Sponsored Project Ref: SR/FTP/ES-61/2014.

REFERENCES

[1] Anderson, J.R., Payne, J.L., Kelsey, D.E., Hand, M., Collins, A.S. and Santosh, M. 2012. High-pressure granulites at the dawn of the Proterozoic. Geology, 40: 431–434.

[2] Amaldev, T., Santosh, M., Li Tang, Baiju, K.R., Tsunogae, T. and Satyanarayanan, M. 2016. Mesoarchean convergent margin processes and crustal evolution: Petrologic, geochemical and zircon U-Pb and Lu-Hf data from the Mercara suture zone, southern India. Gondwana Research, 37: 182–204.

[3] Balaram, V. and Rao, T.G. 2003. Rapid determination of REEs and other trace elements in geological samples by microwave acid digestion and ICP-MS. Atomic Spectroscopy, 24: 206–212.

[4] Barrett, T.J. and Mac Lean, W.H., 1994. Chemostratigraphy and hydrothermal alteration in exploration for VHMS deposits in greenstone and younger volcanic rocks. D.R. Lentz (Ed.), Alteration and Alteration processes associated with Ore forming systems. Geological Association of Canada, short course notes, 11: 433–467.

[5] Bhaskar Rao, Y.J., Chetty, T.R.K., Janardhan, A.S. and Gopalan, K. 1996. Sm-Nd and Rb-Sr ages and P-T history of the Archean Sittampundi and Bhavani layered meta-anorthositic complexes in Cauvery shear zone, South India: evidence for Neoproterozoic reworking of Archean crust. Contributions to Mineralogy and Petrology, 125: 237–250.

[6] Bhutani, R. Balakrishnan, S., Nevin, C.G. and Jeyabal, S. 2007. Sm-Nd isochron ages from Southern Granulite Terrain, South India: age of protolith and metamorphism. Geochimica et Cosmochimica Acta, 71: A89.

[7] Bohlen, S.R. and Mezger, K. 1989. Origin of granulite terrains and formation of lower most continental crust. Science 244, 326–329.

[8] Bose, M.K., Maitra, M. and Das, D. 2001. Structure and petrology of the mafic granulites and associated rocks of the Kanjamalai complex, Salem district, Tamil Nadu. Indian Minerals, 55: 119–132.

[9] Brandt, S., Schenk, V., Raith, M.M., Appel, P., Gerdes, A. and Srikantappa, C., 2011. Late Neoproterozoic P-T evolution of HP-UHT granulites from the Palani hills (south India): New constraints from phase diagram modeling, LA-ICP-MS zircon dating and in-situ EPMA monazite dating. Journal of Petrology, 52: 1813–1856.

[10] Brandt, S., Raith, M.M., Schenk, V., Sengupta, P., Srikantappa, C. and Gerdes, A. 2014. Crustal evolution of the Southern Granulite Terrain, South India: new geochronological and geochemical data for felsic orthogneisses and granites, Precambrian Research, 246: 91–122.

[11] Brown, B., 2007. Metamorphism, plate tectonics and super-continent cycle. Earth Science Frontiers, 14: 1–18.

[12] Braun, I., Raith, M., and Ravindra Kumar, G.R. 1996, Dehydration melting phenomena in leptynitic gneisses and the generation of leucogranites: a case study from the Kerala Khondalite Belt, southern India. Journal of Petrology, 37: 1285–1305.

[13] Cenki, B., Braun, I. and Brocker, M. 2004. Evolution of the continental crust in the Kerala Khondalite Belt, southern most India: evidence from Nd isotope mapping, U-Pb and Rb-Sr geochronology. Precambrian Research, 134: 275–292.

[14] Chacko, T., Kumar, G.R.R. and Newton, R.C., 1987. Metamorphic P-T conditions of Kerala (south India) Khondalite Belt, a granulite facies supracrustal terrain. Journal of Geology, 95, 343-358.

[15] Chacko, T., Kumar, G.R.R., Meen, J.K. and Rogers, J.J.W. 1992. Geochemistry of high grade supracrustal rocks from the Kerala Khondalite Belt and adjacent massif charnockites. Precambrian Research, 55, 469–489.

[16] Chetty, T.R.K. and Bhaskar Rao, Y.J. 2006. The Cauvery shear zone, southern granulite terrain, India: a crustal-scale flower structure. Gondwana Research, 10: 77–85.

[17] Chetty, T.R.K., Yellappa, T. and Santosh, M. 2016. Crustal architecture and tectonic evolution of the Cauvery suture zone, southern India. Journal of Asian Earth Sciences, 130: 166-191.

[18] Choudhary, A.K., Jain, A.K., Sandeep Singh, Mnickavasagam, R.M. and Chandra, K. 2011. Crustal accretion and metamorphism of Mesoarchean granulites in Palghat-Cauvery shear zone, southern India. Journal of Geological of Society of India, 77, 227–238.

[19] Christensen, N.I. and Fountain, D.M. 1975. Constitution of the lower continental crust based on experimental studies of seismic velocities in granulites. Geological Society of America Bulletin, 86: 227–236,

[20] Collins, A.S., Clark, C., Sajeev, K., Santosh, M., Kelsey David, E. and Martin, H. 2007. Passage through India: Mozambique ocean suture, high pressure granulites and Palghat-Cauvery shear zone system. Terra Nova, 19: 41–147.

[21] Collins, A.S., Clark, C., and Plavsa, D., 2014, Peninsula India in Gondwana: the tectonothermal evolution of the southern granulite terrain and its Gondwana counter parts. Gondwana Research, 25: 190–203.

[22] Drury, S.A. and Holt, R.W. 1980. The tectonic framework of the south Indian craton: a reconnaissance involving LANDSAT imagery. Tectonophysics, 65: T1–T5.

[23] Drury, S.A., Harris, N.B.W., Holt R.W., Reeves Smith, G.J. and Wightman, R.T. 1984. The Precambrian tectonics and crustal evolution in south India. Journal of Geology, 92: 3–20.

[24] Dutta, D., Bhui, U.K., Sengupta, P, Sanyal, S. and Mukhopadhyay, D. 2011. Magmatic and metamorphic imprints in 2.9 Ga chromitites from the Sittampundi layered complex, Tamil Nadu, India. Ore Geology Reviews, 40: 90–107.

[25] Frost B.R. and Frost, C.D. 1987, CO_2 melts and granulite metamorphism. Nature, 327: 503–506.

[26] Ghosh, J.G., Maarten J., de Wit and Zartman, R.E. 2004. Age and tectonic evolution of Neoproterozoic ductile shear zones in the southern granulite terrain of India, with implications for Gondwana studies. Tectonics, 23: TC3006.

[27] Glorie, S., De Grave, J., Singh, T., Payne, J.L. and Collins, A.S. 2014. Crustal root of the eastern Dharwar craton: zircon U-Pb age and Lu-Hf isotopic evolution of the East Salem Block, southeast India. Precambrian Research, 249: 229–246.

[28] Gopalakrishnan, K. 1994. An overview of southern granulite terrain, India-constraints in reconstruction of Precambrian assembly of Gondwana land. Gondwana Nine, 2, Oxford and IBH Publishers, 1003–1026.

[29] GSI., 2006. Geology and mineral resources of states of India, Tami Nadu and Pondicherry. Geological Survey of India, Miscellaneous Publication, No. 30.

[30] Hansen, E.C, Newton, R.C. and Janardhan A.S. 1984. Fluid inclusion in rocks from the amphibolite-facies gneiss to charnockite progression in southern Karnataka, India: Direct evidence concerning the fluids of granulite metamorphism. Journal of Metamorphic Geology, 2: 249–264.

[31] Harley, S.L. 2004. Extending of our understanding of ultrahigh temperature crustal metamorphism. Journal of Mineralogical and Petrological Sciences, 99: 140–158.

[32] Harris, N.B.W., Holt, R.W. and Drury, S.A. 1982. Geobarometry, geothermometry and Late-Archean geotherms from the granulite facies terrain of south India. Journal of Geology, 90: 509–527.

[33] Harris, N.B.W, Santosh, M. and Taylor, P.N. 1994. Crustal evolution in south India: constraints from Nd-isotopes. Journal of Geology, 102: 139–150.

[34] Irvine, T.N. and Baragar, W.R.A. 1971. A guide to the chemical classification of common volcanic rocks. Canadian Journal of Earth Science, 8: 523–548.

[35] Ishii, S., Tsunogae, T. and Santosh, M. 2006. Ultra-high temperature metamorphism in Achankovil zone: implication for correlation of crustal blocks in south India. Gondwana Research, 10: 99–114.

[36] Janardhan, A.S., Jayananda, M. and Sahnakara, M.A., 1994, Formation and Tectonic evolution of Granulites from the Biligiri Rangan and Nilgiri Hills, south India: geochemical and isotopic constraints. Journal of Geological Society of India, 44, 27–40.

[37] Kay, S.G. and Kay, R.W. 1983. Thermal history of deep crust inferred from granulite xenoliths. American Journal of Science, 283: 486–513.

[38] Jensen, L.S. 1976. A new cation plot for classifying sub-alkalic volcanic rocks. Ontario Geological Survey Miscellaneous paper, 66.

[39] Johnson, T.E., Clark, C., Taylor, R.J.M., Santosh, M. and Collins, A.S. 2015. Prograde and retrograde growth of monazite in migmatites: an example from the Nagercoil Block, southern India. Geoscience Frontiers, 6: 373–387.

[40] Koizumi, T., Tsunogae, T., Santosh M. and Chetty, T.R.K. 2014. Petrology and zircon U-Pb geochronology of metagabbros from a mafic-ultramafic suite at Aniyapuram: Neoarchean to Early-Paleoproterozoic convergent margin magmatism and Middle-Neoproterozoic high-grade metamorphism in southern India. Journal of Asian Earth Sciences, 95: 51–64.

[41] Moses, B.V.C., Ram Mohan, V., and Yoshida, M. 1999. Geochemical characteristics of mafic granulites and associated websterites from the Sittampundi complex, south India. Journal of Geosciences, Osaka University, 42, 215–225.

[42] Mukhopadhyay, B. and Bose, M.K. 1994. Transitional granulite-eclogite facies metamorphism of basic supracrustal rocks in a shear zone complex of the Precambrian shield of south India. Mineralogical Magazine, 58, 97–118.

[43] Mullen, E.D. 1983. $MnO/TiO_2/P_2O_5$ a minor element discriminations for basaltic rocks of oceanic environments and its implications for petrogenesis. Earth and Planetary Science Letters, 62: 53–62.

[44] Nandakumar, V. and Harley S.L. 2000. A reappraisal of the pressure-temperature path of granulites from the Kerala Khondalite Belt, southern India. Journal of Geology, 108: 687–703.

[45] Nishimiya, Y., Tsunogae, T. and Santosh, M. 2010. Sapphirine + quartz corona around magnesian ($X_{Mg} \sim 0.58$) staurolite from the Palghat-Cauvery suture sone, southern India: evidence for high-pressure and ultrahigh-temperature metamorphism within the Gondwana suture. Lithos, 114: 490–502.

[46] Noack, N.M., Kleinschrodta, R., Kirchenbaura, M., Fonsecab, R.O.C. and Munker, C. 2013. Lu-Hf isotope evidence for Paleoproterozoic metamorphism and deformation of Archean oceanic crust along the Dharwar craton margin, southern India. Precambrian Research, 233, 206–222.

[47] Newton, R.C., Smith, J.V. and Windley, B.F. 1980. Carbonic metamorphism, granulites and crustal growth. Nature, 288: 45–49.

[48] Pearce, J.A. 1980. Geochemical evidence for genesis and eruptive setting of lavas from Tethyan ophiolites. In: Panayiotou, A. (Ed.), Ophiolites. Geological Survey Department, Cyprus, pp. 261–272.

[49] Pearce, J.A. 1982. Trace element characteristics of lavas from destructive plate boundaries. In: Thorpe, R.S. (Ed.), Andesites. Wylie and Sons, pp. 525–548.

[50] Percival, J.A. 1994. Archean high-grade metamorphism. Developments in Precambrian Geology, Archean crustal evolution edited by K.C. Condie, v.11: 357–410.

[51] Peucat, J.J., Mahabhaleswar, B. and Jayananda, M. 1993. Age of younger tonalitic magmatism and granulite metamorphism in the south India transition zone (Krishnagiri area): comparison with older peninsular gneisses from Hassan-Gorur area. Journal of Metamorphic Geology, 11: 879–888.

[52] Plavsa, D., Collins, A.S., Foden, J.F., Kropinski, L., Santosh, M., Chetty, T.R.K. and Clark, C. 2012. Delineating crustal domains in Peninsular India: age and chemistry of orthopyroxene-bearing felsic gneisses in the Madurai Block. Precambrian Research, 198-199: 77–93.

[53] Plavsa, D., Collins A.S., Payne, J.L., Foden, J.D., Clark, C. and Santosh, M. 2014. Detrital zircons in basement metasedimentary protoliths unveil the origins of southern India. Geological Society of America Bulletin, 126: 791–812.

[54] Prakash, D., 2010, New SHRIMP U-Pb zircon ages of the metapelitic granulites from NW of Madurai, southern India. Journal of Geological Society of India, 76: 371–383.

[55] Praveen, M.N., Santosh, M., Yang, Q.Y., Zhang, Z.C., Huang, H., Singanenjam, S. and Sajinkumar, K.S. 2013. Zircon U-Pb geochronology and Hf isotope of felsic volcanics from Attappadi, southern India: implications for Neoarchean convergent margin tectonics. Gondwana Research, 26: 907–924.

[56] Raith, M., Karmakar, S. and Brown, M. 1997. Ultra-high-temperature metamorphism and multistage decompressional evolution of sapphirine granulites from the Palani Hills ranges, southern India. Journal of Metamorphic Geology, 15: 379–399.

[57] Raith, M., Srikantappa, C., Buhl, D. and Kuhler, H. 1999. The Nilgiri enderbites, south India: nature and age constraints on protolith formation, high-grade metamorphism and cooling history. Precambrian Research, 98: 129-150.

[58] Rajesh, H.M. and Santosh, M., 2004, Charnockitic magmatism in southern India. Journal of Earth System Science, 113: 565–585.

[59] Rajesh, H.M. 2007. The petrogenetic characterization of intermediate and silicic charnockites in high-grade terrains: a case study from southern India. Contributions to Mineralogy and Petrology, 154: 591–606.

[60] Rajesh, H.M. 2012. A geochemical perspective on charnockite magmatism in Peninsular India. Geoscience Frontiers, 3: 773–788.

[61] Ramakrishnan, M. 1993. Tectonic evolution of granulite terrains of southern India. Geological Society of India Memoir, 25, 35–44.

[62] Ramakrishnan, M. and Vaidyanathan, R. 2008. Geology of India, Geological Society of India, Bangalore, Vol. 1.

[63] Ratheesh Kumar, R.T., Santosh, M., Yang, Q.Y., Ishwar-Kumar, Song Chen, N. and Sajeev, K., 2016. Archean tectonics and crustal evolution of the Biligiri Rangan Block, Southern India. Precambrian Research, 275: 406–428.

[64] Ravindra Kumar, G.R. and Sreejith, C., 2016. Petrology and geochemistry of charnockites (felsic ortho-granulites) from the Kerala Khondalite Belt, Southern India: Evidence for intra-crustal melting, magmatic differentiation and episodic crustal growth. Lithos, 262: 334–354.

[65] Rudnick, R.L., McLennan, S.M. and Taylor, S.R. 1985. Large ion lithophile elements in rocks from high-pressure granulite facies terrains. Geochimica et Cosmochimica Acta 49: 1645–1655.

[66] Rudnick, R.L. and Gao, S., 2003. The Composition of the continental crust. In: Holland, H.D. and Turekian, K.K., Eds., Treatise on Geochemistry, Elsevier-Pergamon, Oxford, Vol. 3: 1–64.

[67] Saitoh, Y., Tsunogae, T., Santosh, M., Chetty, T.R.K., and Horie, K. 2011. Neoarchean high-pressure metamorphism from the northern margin of the Palghat-Cauvery suture zone, southern India: Petrology and zircon SHRIMP geochronology. Journal of Asian Earth Sciences, 42: 268–285.

[68] Sajeev, K., Windley, B.F., Connolly, J.A.D. and Kon, Y. 2009. Retrogressed eclogite (20 kbar, 1020ºC) from the Neoproterozoic Palghat-Cauvery suture zone, southern India. Precambrian Research, 171, 23–36.

[69] Samuel, V.O., Santosh, M., Liu, S., Wang, W. and Sajeev, K. 2014. Neoarchean continental growth through arc magmatism in the Nilgiri Block, Southern India. Precambrian Research, 245: 146–173.

[70] Santosh, M., Yokoyama, K., Sekhar, B.S., and Rogers, J.J.W., 2003. Multiple tectonothermal events in the granulite blocks of southern India revealed from EPMA dating: implications on the history of supercontinents. Gondwana Research, 6: 29–63.

[71] Santosh, M. and Sajeev, K. 2006. Anticlockwise evolution of ultrahigh-temperature granulites within continental collision zone in southern India. Lithos, 92: 447–464.

[72] Santosh, M. and Omori, S., 2008. CO_2 flushing: a plate tectonic perspective. Gondwana Research, 13: 86-102.

[73] Santosh, M., Maruyama, S. and Sato, K. 2009. Anatomy of a Cambrian suture in Gondwana: Pacific-type orogeny in southern India? Gondwana Research, 16: 321–341.

[74] Santosh, M., Xiao, W.J., Tsunogae, T., Chetty, T.R.K., and Yellappa T. 2012. The Neoproterozoic subduction complex in southern India: SIMS zircon U-Pb ages and implications for Gondwana assembly. Precambrian Research, 192, 190–208.

[75] Santosh, M., Shaji, E., Tsunogae, T., Ram Mohan, M., Satyanarayanan, M., and Horie, K. 2013. Neoarchean suprasubduction zone ophiolite from Agali hill, southern India: petrology, zircon SHRIMP U-Pb geochronology, geochemistry and tectonic implications. Precambrian Research, 231: 301–324.

[76] Santosh, M., Yang, Q.Y., Ram Mohan, M., Tsunogae, T., Shaji, E., and Satyanarayanan, M. 2014. Cryogenian alkaline magmatism in the Southern Granulite Terrain, India: petrology, geochemistry, zircon U-Pb ages and Lu-Hf isotopes. Lithos, 208-209: 430–445.

[77] Santosh, M., Nan Hu, C., Fang He, X., Shan Li, S., Tsunogae, T., Shaji, E. and Indu, G. 2017. Neoproterozoic arc magmatism in the southern Madurai Block, India: subduction, delamination, continental outbuilding, and the growth of Gondwana. Gondwana Research, 45, 1–42.

[78] Sato, K., Santosh, M., Tsunogae, T., Chetty, T.R.K. and Hirata, T. 2011. Subduction-accretion-collision history along the Gondwana suture in southern India: a laser ablation ICP-MS study on zircon chronology. Journal of Asian Earth Sciences, 40: 162–171.

[79] Shaji, E., Santosh M., Fang He, X. , Rui Fan, H., Dhanil Dev, S.G., Yang, K.F., Thangal, M.K. and Pradeep Kumar, A.P. 2014. Convergent margin processes during Archean-Proterozoic transitionin southern India: Geochemistry and zircon U-Pb geochronology of gold-bearing amphibolites, associated metagabbros, and TTG gneisses from Nilambur. Precambrian Research, 250, 68–96.

[80] Sheraton, J.W. and Collerson, K.D. 1984. Geochemical evolution of Archean granulite facies gneisses in the Vestfold Block and comparison with other Archean gneissic complexes in the East Antarctica shield. Contributions to Mineralogy and Petrology, 87: 51–64.

[81] Shervais, J.W. 1982. Ti-V plots and the petrogenesis of ophiolitic lavas. Earth and Planetary Science Letters, 59: 101–118.

[82] Shu, L., Jinhai Yu, Charvet, J., Charvet, S.L, Sang, H., and Zhang, R. 2004, Geological, geochronological and geochemical features of granulites in the Eastern Tianshan, NW China. Journal of Asian Earth Sciences, 24 (1): 25–41.

[83] Srikantappa, C., Raith, M., and Touret, J.L.R. 1992. Syn-metamorphic high density carbonic fluids in the lower crust: evidence from Nilgiri granulite, south India. Journal of Petrology, 33: 733–760.

[84] Sun, S.S. and Mc Donough, W.F. 1989. Chemical and isotope systematics of oceanic basalts: implications for mantle composition and processes. In: Saunders, A.D., Norry, M.J. (Eds.), Magmatism in the Ocean Basins, Geological Society of London Special Publications, 42: 313–345.

[85] Teale, W., Collins, A., Foden, J., Payne, J., Plavsa, D., Chetty, T.R.K., Santosh, M. and Fanning, M. 2011. Cryogenian (~830Ma) mafic magmatism and metamorphism in the northern Madurai Block, Southern India: a magmatic link between Sri Lanka and Madagascar. Journal of Asian Earth Sciences, 42: 223–233.

[86] Tomson, J.K., Bhaskar Rao, Y.J., Vijaya Kumar, T. and Mallikharjuna Rao, J. 2006. Charnockite genesis across the Archean-Proterozoic terrain boundary in the south Indian granulite terrain: constraints from major-trace element geochemistry and Sr-Nd isotopic systematics. Gondwana Research, 10: 115–127.

[87] Tomson, J.K., Bhaskar Rao, Y.J., Vijaya Kumar, T., and Choudhary, A.K. 2013. Geo-chemistry and neodymium model ages of Precambrian charnockites, southern granulite terrain, India: constraints on terrain assembly. Precambrian Research, 227: 295–315.

[88] Toruet, J.L.R., Santosh, M. and Huizenga, J.M. 2016. High temperature granulites and super continents. Geoscience Frontiers, 7: 101–113.

[89] Tsunogae, T. and Santosh, M. 2006. Spinel-saphirine-quartz bearing composite inclusions within garnet from an ultrahigh-temperature pelitic granulite: implications for metamorphic history and P-T path. Lithos, 92: 524–536.

[90] Tsunogae, T., Santosh, M. and Dubessy, J. 2008. Fluid characteristics of high- to ultrahigh-temperature metamorphism in southern India: a quantitative Raman spectroscopic study. Precambrian Research, 162: 198–211.

[91] Weaver, B.L. 1980. Rare-Earth Element Geochemistry of Madras Granulites. Contributions to Mineralogy and Petrology, 71: 271–279.

[92] Winchester, J.A. and Floyd, P.A. 1977. Geochemical discrimination of different magma series and their differentiation products using immobile elements. Chemical Geology, 20: 325–343.

[93] Yellappa, T., Chetty, T.R.K., Tsunogae, T. and Santosh, M. 2010. The Manamedu Complex: geochemical constraints on Neoproterozoic suprasubduction zone ophiolite formation within the Gondwana suture in southern India. Journal of Geodynamics, 50: 268–285.

[94] Yellappa, T., Santosh, M., Chetty, T.R.K., Sanghoon Kwon, Chansoo Park, Nagesh, P., Mohanty D.P. and Venkatasivappa, V. 2012. A Neoarchean dismembered ophiolite complex from southern India: geochemical and geochronological constraints on its suprasubduction origin. Gondwana Research, 21: 246–265.

[95] Yellappa, T., Venkatasivappa, V., Koizumi, T., Chetty, T.R.K., Santosh, M. and Tsunogae, T. 2014. The mafic-ultramafic complex of Aniyapuram, Cauvery Suture Zone, Southern India: petrological and geochemical constraints for Neoarchean suprasubduction zone tectonics. Journal of Asian Earth Sciences, 95: 81–98.